Wiley
International Journal of Energy Research
Volume 2025, Article ID 1963336, 22 pages
https://doi.org/10.1155/er/1963336

WILEY

Review Article

Thermal Conductivity of BN-Based Polymer Composites for Thermal Interface Management: Progress and Applications

Muneeb Ur Rehman,[1,2] **Muhammad Faheem Maqsood**,[3,4] **Laraib Sajjad**,[5]
Aamir Nadeem,[1] **Ehsan Elahi**,[6] **Mohammed A. Assiri**,[7] **Karim Khan**,[8]
Shania Rehman,[5] **Malik Abdul Rehman**,[9] **Qiaohuan Cheng**,[2] and
Muhammad Farooq Khan[4]

[1]*Institute of Metallurgy and Materials Engineering, Faculty of Chemical and Materials Engineering, University of the Punjab, Lahore 54590, Pakistan*
[2]*School of Materials Science and Engineering, Henan University of Technology 450001, Zhengzhou, China*
[3]*Materials Research Center (MRC), College of Arts and Sciences, American University of Sharjah, Sharjah 26666, UAE*
[4]*Department of AI Convergence Electronic Engineering, Sejong University 05006, Seoul, Republic of Korea*
[5]*Semiconductor Systems Engineering, Sejong University, Seoul 05006, Republic of Korea*
[6]*Department of Physics and Astronomy, Sejong University 05006, Seoul, Republic of Korea*
[7]*Department of Chemistry, College of Science, King Khalid University, Abha 61413, Saudi Arabia*
[8]*School of Electrical Engineering and Intelligentization, Dongguan University of Technology, Dongguan 523808, China*
[9]*Department of Chemical Engineering, New Uzbekistan University, Tashkent 100007, Uzbekistan*

Correspondence should be addressed to Malik Abdul Rehman; m.abdul@newuu.uz,
Qiaohuan Cheng; qiaohuan_cheng@haut.edu.cn, and Muhammad Farooq Khan; mfk@sejong.ac.kr

Received 2 November 2024; Revised 4 June 2025; Accepted 4 August 2025

Academic Editor: Chaofan Sun

Advanced electronic technology significantly relies on the superior heat-conducting materials to efficiently manage the heat generated by circuit assemblies. Effective thermal management is essential to ensure the reliability, efficiency, and durability of electronic devices. The thermal conductivity (TC) of polymers can be improved by initiating several nanofillers and constructing a three-dimensional (3D) conductive path for phonon transfer. In this review, we discussed the synthesis of boron nitride (BN), the thermal characteristics of BN, and BN filler in polymer matrix for enhanced TC. It is summarized that the TC of the polymer composites could be enhanced in case when matrix is added with BN nanosheets (BNNSs) through bidirectional freezing, hot pressing, roll cutting, and making the 3D structure of reinforcement, making it suitable for the applications of electronic packaging. Also, hybrid fillers such as short carbon fiber, BN nanotubes (BNNTs), and nanosheets may construct a highly conductive path for phonon transfer. In addition, we highlighted the challenges and provided the prospects of BN nanostructures in various applications of thermal management to enhance the functional capability of equipment and electronic gadgets.

Keywords: boron nitride; boron nitride nanosheets; polymer composites; thermal conductivity; thermal interface management

1. Introduction

The electrical technology provokes faster electronic communication devices and gadgets that generate noticeable heat content, and its dissipation is a crucial factor [1, 2]. Modern electronic devices are consistently leading towards miniaturization and functionalization, and their main challenge is heating transference [3, 4]. The rapid advancement of 5G technology and high-power electronic devices has significantly increased the demand for efficient thermal management solutions. Those composites/materials that offer high thermal conductivity (TC) while upholding tremendous electrical insulation are essential for efficient heat dissipation in 5G base stations and other high-power-density systems [5, 6]. The operation of electronic devices could be smooth by dissipating heat at a moderate rate through a heat-sinking mechanism, but sometimes weak thermal linkage between heat sink and the device restricts heat dissipation [7]. To cater this, thermal interface materials (TIMs) have been engaged to minimize thermal resistance by building conducting paths between asperities [8]. The polymer resins are extensively used as TIMs due to their high electrical resistivity, low cost, and good mechanical properties. However, their intrinsically low TC (0.1–0.5 W/m.K) restrains their effectiveness in thermal management applications [9].

Despite challenges, thermally conductive polymer composites show a great potential in several applications of stretchable networks, thermal management, and aerospace [10, 11]. Therefore, the recent research is focused to predict the properties of particle-reinforced composites and ceramics to develop polymers with metal-like TC for advanced thermal management solutions [12–14]. For example, slim light-emitting diode (LED) TVs contain various miniaturized LEDs in a single panel, and generation of heat due to emissions can cause several problems for the efficiency of LEDs, for example, color shifts, reduced light output, and their longevity [15]. The heat sinks do not efficiently dissipate heat because of thermal barrier resistance; enhanced thermal conductive materials are placed between heat sinks and the device interface to dissipate thermal energy efficiently [16]. Effective thermal management is influential for battery performance and safety purposes in electric vehicles. While excessive heat is generated during charging and discharging, reducing the battery lifetime and increase fire risk [17]. The cooling strategies including air, liquid, and phase change material (PCM) systems have been explored where PCMs offer lightweight, energy-efficient, and uniform thermal regulation but cost low TC [17, 18]. To address this, researchers have integrated thermally conductive additives such as metal fins, foams, and expanded graphite into PCMs. Novel approaches like central heat sinks have also been proposed to address heat accumulation in battery cores [19].

Moreover, 5G communication technology uses ultrahigh-speed signals of millimeter waves, and loss in microwave radiation causes heat. To prevent signal loss, 5G communication technology demands a very low dielectric constant and to minimize signal attenuation in high-frequency communications [20, 21].

Boron nitride (BN) is a ceramic compound of boron and nitrogen with high TC, high thermal expansion coefficient, and good dimensional strength [22, 23]. BN has strong covalent bonding and found in different variants like sheets, nanotubes, and particles having similarities with carbon-based microstructures [24]. Cubic BN has a diamond-like structure, h-BN has hexagonal (honeycomb-like) structure whereas the w-BN seems like a hexagonal diamond [25–27]. To determine the stress and mechanical properties at nanoscale level, nanoindentation is being used to create trenches on BN surface to boost the thermal contact of BN and polymer matrix for rapid heat transfer [28–30]. The h-BN being the most stable allotrope of BN, and suitable as filler to elevate the TC of polymer matrix, improving high-temperature oxidation resistance, and optimize mechanical properties [31, 32]. Having wide energy band gap (5.9 eV) of BN, the BN/polymer composites have become more auspicious for electronic packaging applications. The electrical resistance of the material used for electronic application must be in the range of 10^{11}–10^{24} Ω-cm [33]. Therefore, BN having a low dielectric constant of 34.8 and excellent temperature resistance is appropriate for thermal management applications [34]. Factors include significant interfacial thermal resistance (ITR), the inherently low TC of the filler material, and the limited thermal transfer efficiency (TTE) per unit mass of the filler, hinders effective heat flow within the materials/composites, thereby, reducing the overall thermal performance [35].

Instead, the TC can be significantly improved by using a hybrid filler, where the mixture of two fillers (hybrid filler) produces a collaborative effect that exceeds the possible performance of a single filler. The production of such nanocomposites is challenging because of repulsion between inorganic filler and organic polymer. To overcome this problem several techniques have been adopted including surface modification by surfactants, adhesive agents, and selective functional polymers [36–38].

To avoid agglomeration of filler particles, it is suggested to enhance matrix–filler interaction while diminishing filler–filler interaction by different strategies, such as using particles of different shapes or functionalizing the surface of particle [39]. The self-agglomeration of a single nanofiller is minimized by choosing two fillers of different morphology [40]. A filler content of less than 50 vol.% does not improve thermal efficiency [41]. Fillers are available in 3D, 2D, 1D, and 0D forms. Surprisingly, the area of contact decreases with increasing filler dimensions [42, 43]. Since ITR is essential in reducing TTE, the 3D interfacial filler composition is highly suitable for enhancing TC in composites [44, 45]. The dispersion of hybrid fillers in a polymeric matrix can be altered due to their dimensional orientation. Recent research revealed that spherical fillers are uniform to 1D or 2D fillers due to less contact area. The dispersion issue of 2D fillers has been resolved by their hybridization with a filler having better dispersion ability [46, 47]. This review demonstrates and summarizes the emerging techniques for enhancing the TC of various polymers by hybrid loading BN with other fillers.

2. Synthesis and Thermal Characteristics of BN

2.1. Synthesis of BN. BN is being fabricated and synthesized in various forms like 1D BN nanotubes (BNNTs), 2D BN nanosheets (BNNSs), BN nanoribbon (BNNRs), and BN nanoflakes (BNNFs). BN is synthesized using different boron and nitrogen precursors; the most common are boron powder and ammonia gas, while boric acid and ammonia gas are popular precursors for creating BN [48]. BNNS is a hexagonal BN (hBN) layered structure possessing excellent mechanical and thermal properties but large energy band gap for electrical resistivity. Since BNNSs can be synthesized by using different approaches, among which commonly practiced are chemical vapor deposition (CVD), laser arc ablation, liquid phase exfoliation (LPE), and ball milling as shown in Figure 1a–d [49–52].

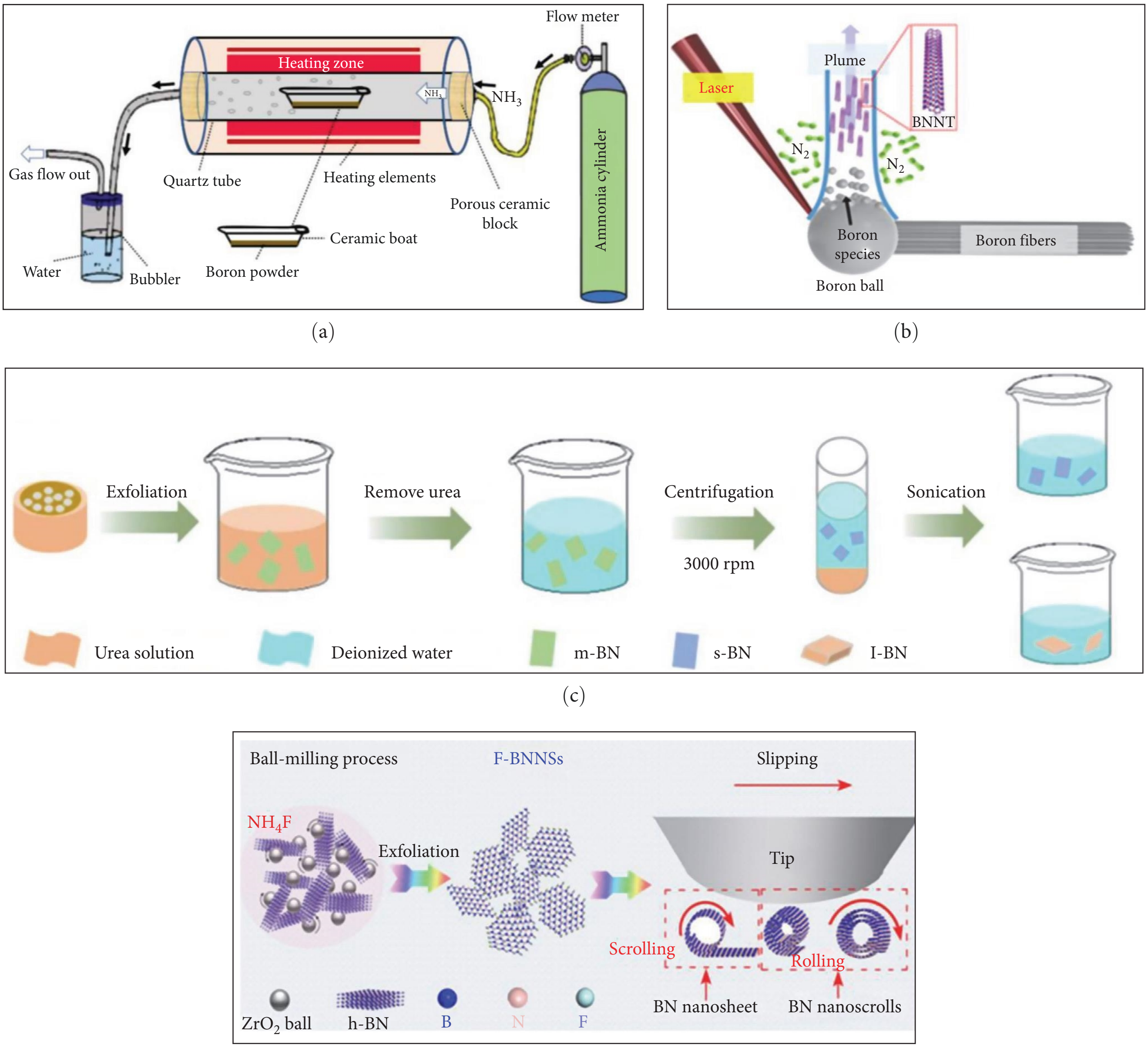

(a) (b)

(c)

(d)

Figure 1: (a) Chemical vapor deposition [49], Copyright 2020 Elsevier. (b) Laser arc ablation [50], Copyright 2019 Springer Nature. (c) Liquid phase exfoliation [51], Copyright 2019 IOP. (d) Different methods to produce BN by ball milling method [52], Copyright 2020 ACS.

In addition, ball milling can be employed efficiently and beneficially for scalable exfoliation of layered materials.

Recently, Lie et al. [53] employed ball milling process to prepare a few layered BNNSs from bulk h-BN by applying ammonia borane as milling agent. This method is risky for the integrity of BNNSs, which can create defects in the crystal structure. Nonetheless, CVD is a readily available way for producing 2D materials with a large surface area [49]. Whereas the BNNSs can be grown on substrates like Cu, Fe, etc. [54, 55]. Added to this, Aamir and co-workers successfully produced BNNSs of 5–11 nm thickness with boron powder (1–2 µm) and NH_3 gas in a CVD setup, which was performed at 1200°C for 1 h [49]. However, CVD provides good quality BNNSs at optimum reaction conditions, but low yield and high energy usage limit its commercial adoption. The LPE is the most suitable technique in various aspects of BNNS synthesis [56]. hBN can directly produce a few layered BNNSs through sonication in various chemical solvents such as isopropyl alcohol (C_3H_8O), dimethyl sulfoxide (C_2H_6OS), N-methyl pyrrolidone (C_5H_9NO), and thionyl chloride ($SOCl_2$). These solvents have enough surface energy that is desired for the exfoliation of bulk h-BN. Although the LPE method faces of limitations such as low yield, slow processing, and re-agglomeration of exfoliated BNNSs, these challenges can be mitigated through functionalization. The surface modification enhances the dispersion stability of BNNSs by improving their compatibility with polymer matrices. Functionalization can be done through various solutions; for example, Zhao et al. [57]

used tannic acid for exfoliation and functionalization of BNNSs and reported a yield of 42.2%. Also, in 1995 the pure BNNTs were first made by Chopra et al. [58] with arc discharge method. The BNNTs and its composites are being widely used in biomedical fields, and nanodevices as well as hydrogen uptake applications [59] due to their remarkable TC, piezoelectricity, and Young's modulus [60–62]. Moreover, generally BNNTs have been synthesized by several methods like CVD, ball milling, boron ink annealing, laser ablation, and arc-jet plasma [63–67]. However CVD is more applicable method for producing BNNTs in quantity and quality. The systematic investigation by Zhuang et al. [68] has been carried out to synthesize the BNNTs on a stainless steel surface by ball milling followed by an annealing process using N_2/H_2 gas at 1200°C. Interestingly, the gas flow rate and precursor ratio determined the morphology, yield, and size of the BNNTs. On the other hand, Ahmad et al. [69] produced human hair-like BN nanofibers by a mixture of boron, magnesium oxide, and iron oxide powders using CVD technique. Furthermore, this group grew the bamboo-like structure BNNTs by argon-supported thermal CVD. However, the acquired BNNTs showed a pattern of straight, nearly straight, and curved shapes with a diameter of 20–80 nm [70].

2.2. TC of BN. TC originates from phonon conduction, where the phonons are quanta of vibrational energy [71]. On providing heat, surface particles of the material undergo vibrations. During the vibrating phenomenon, heat transfers to the nearest particle. TC k (W/m-k) defines thermal conduction, thereby, the thermal conduction rate depends on the difference in temperature between opposite faces. So, the higher the temperature difference leads to higher thermal conduction. TC (k) can be determined as [72]:

$$k = \alpha . Cp\, \rho \tag{1}$$

where k is the thermal conductivity, Cp is the specific heat, ρ is the density, and a is the thermal diffusivity.

The addition of fillers such as carbon nanotubes [73, 74], metal fillers [75], and ceramic fillers [76, 77] in polymer matrices increases the TC. The h-BN imparts TC to polymer as of its high TC (400 W/m.K) at ambient temperature. The recent studies show that TC increased by reducing the phonon–phonon scattering mechanism [78]. In case, BN is highly suggested for internal dielectric material in batteries due to its remarkable TC and electrical resistivity. The TC of BN composites is drastically influenced by amount and size/morphology of filler. The smaller BN filler particles support to a greater number of interfaces, which increases phonon scattering. Consequently, the overall TC is reduced compared to systems with large particle sizes of filler that offer fewer interfacial boundaries [79]. Another report shows that TC increases by adding micrometer length BNNSs in polymer matrix [80, 81]. For instance, Hatsuo et al. [82] stated that the TC of polybenzoaxine (C_8H_7NO) is improved 30 times higher with the addition of 225 μm lateral size BNNSs with a ratio of 78.5 vol.%. However, processing parameters affect the integrity of the composite, that is, high percentage of filler can cause the porosity. Therefore, polymer and BNNSs composite are efficiently produced by sonication [83], ball milling [84], pressing [85], and mixing [86], significantly impact the distribution of BN filler in the polymer matrix.

In current literature, BNNSs and BNNTs-related nanomaterials perfectly accumulate in polymer matrix due to their high surface energy [87]. Mackay et al. [88] presented that good dispersion occurs when the nanoparticle radius is smaller than the polymer radius of gyration. As, composite in which polystyrene (PS) nanoparticles are blended into PS, a miscible system is achieved when the nanoparticle radius is 1–4 times less than the PS radius of gyration. It is stated that good dispersion is required in composites at higher volume percentage of filler, and dispersion impacts little with less filler loading [89, 90]. Fillers do not accumulate at very low filler loading [91]. Thus, it is more profound to examine the interconnectivity among filler particles and its influence on TC, instead of simply considering the number of fillers. Once strong interconnections are established between particles, a three-dimensional (3D) network can be developed, which significantly improves TC through more competent phonon transport [92].

3. BN as a Filler in Polymer Matrix for Enhancing TC

There are numerous approaches that have been reported to increase the TC of polymer composites/compounds. Some important routes and approaches are mentioned below.

3.1. BN Filled Composites. Liu et al. [93] investigated that the TC of composite film is substantially augmented with the addition of short carbon fibers (SCF) and BN to polydimethylsiloxane (PDMS) matrix by creating efficient conductive path in PDMS. A schematic drawing of the synthesis method of SCF/BN/PDMS composite is shown in Figure 2a.

The base and curing agents (ratio; 10:1) of PDMS were put together and blended for 10 min. Then, SCF and BN were put into this solution and stirred for 20 min to get a homogenous mixture. The mixture was vacuumed in a tank for defoaming and subsequently put onto a polytetrafluoroethylene (PTFE) template by drop casting, and the film was produced through the spin-coating technique. This film was cured for 30 min. A total of six films were prepared by changing the composition of filler contents. The TC of neat PDMS is 0.21 W/m.K, which increased with the amount of filler loaded into a composite. The TC of the composite reached up to 0.87 W/m.K with just a 15 wt.% addition of SCF.

The SCF merged each other and made a conductive path for phonon (see Figure 2b). The addition of BN multiplied the TC of composite, which concluded that the higher BN content leads to higher TC. Different compositions of filler were tried, and the optimized TC value has been found ~ 2.29 W/m.K for 15 wt.% SCF/20 wt.% BN /PDMS composition. The cross-sectional images of PDMS and PDMS composite films were obtained by SEM, as shown in Figure 2c–f. As given the microstructure of the films changes noticeably with the addition of SCF and BN. The SEM image of the pure PDMS film appears smooth (Figure 2c), while SCFs are clearly visible on the cross section when 15 wt.% SCF is incorporated (Figure 2d). With

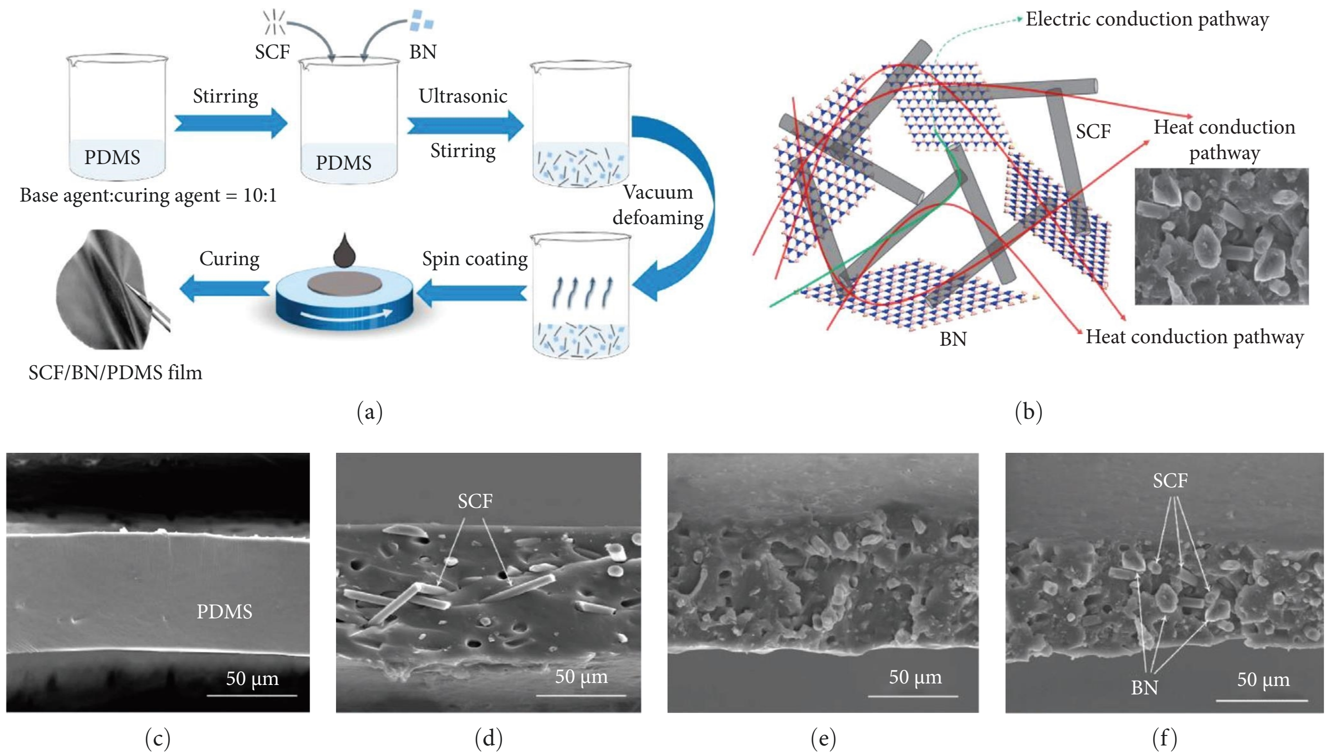

Figure 2: (a) Simplified diagram of synthetic process of SCF/BN/PDMS, (b) thermal and electrically conductive diagram of SCF/BN/PDMS composites. The cross-section SEM images of (c) PDMS, (d) 15%SCF/PDMS, (e) 15%SCF/5%BN/PDMS, and (f) 15%SCF/20%BN/PDMS [93]. Copyright 2021 Elsevier.

the further addition of BN particles (5%) to the SCF/PDMS composite film, the BN particles are uniformly distributed across the cross section (Figure 2e). By increasing the BN content (15%) in the composites resulting in a higher number of BN particles observed (Figure 2f).

The development of nanocomposites aimed at effective heat dissipation makes them readily acceptable for extensive applications. Fabrication of PS loaded with h-BN has excellent thermal transfer properties. Han et al. [94] reported that BN-based carboxylate PS-coated hydroxylated (OH/PS–COOH) nanocomposite has excellent thermal and mechanical characteristics for thermal management applications. Han et al. claimed to enhance the TC of BN-based OH/PS–COOH nanocomposite to ~1.131 W/m.K at 12 wt.% addition of BN–OH. This nanocomposite has outstanding mechanical properties. In situ polymerization was used to construct the BN-based OH/PS–COOH nanocomposite.

The synthesis of (BN–OH) starts with hydroxylation and exfoliation of BNNSs involved molten hydroxide-assisted exfoliation of BNNSs and hydroxylation (see Figure 3a). For peeling and hydroxylation of BNNSs, 2.0 g BNNSs, 4.32 g KOH, and 5.68 g NaOH were blended through ball milling and heating at 180°C for 2 h. The ball-milled output is seated in deionized water overnight before collection whereas the final product was gathered after filtration.

The suspension polymerization prepared PS–COOH. 9 g styrene, 3 g acrylic acid, and 0.2 g of gelatin were mixed in DI water (200 ml). The above mixture was homogenized through ultra-sonication at 90 W for 40 min in the cooling bath and continue the stirring for 4 h at 500 rpm, during which 0.57 g of 2,2′-Azobis (isobutyronitrile) (AIBN) was added. The resultant obtained material was washed with H_2O and C_2H_5OH and put in vacuum to dry it for 24 h at 60°C to attain PS–COOH nanospheres.

Suspension polymerization was used to synthesize the BN-based OH/PS–COOH nanocomposite. BN–OH powder and styrene were used as precursors as shown in Figure 3b. This process is almost the same as preparing PS–COOH. 1.0 g BN–OH powder, 9 g Styrene, 3 g acrylic acid, and 0.2 g of gelatin were mixed in deionized water (200 ml) through the ultrasonication process in cooling bath for 40 min at 90 W. This mixture was stirred for 4 h at 500 rpm with the addition of 0.57 g AIBN under the presence of N_2. The output was washed with water, ethanol, and subsequent vacuum drying to attain the BN-based OH/PS–COOH nanocomposite. This nanocomposite was reshaped in the form of film (0.2 mm thickness) by pressing through a molding machine at 170°C and 40 MPa. Another composite was prepared by hot-pressing of PS/BN blend to compare results. So, BN-based OH/PS–COOH nanocomposites were prepared using an in-situ polymerization process and styrene monomer, acrylic acid, and BNNSs as reactants. The mechanism in this process was to build a macromolecular chain on the BN–OH surface through polymerization and subsequent molding by hot-press. The optimized quantity of filler measured was 12 wt.%.

Figure 3c indicates that PS–COOH powder has various nano-spheres with 200 nm diameter. While Figure 3d shows boundaries of exfoliated BN are apparent, and some are folded.

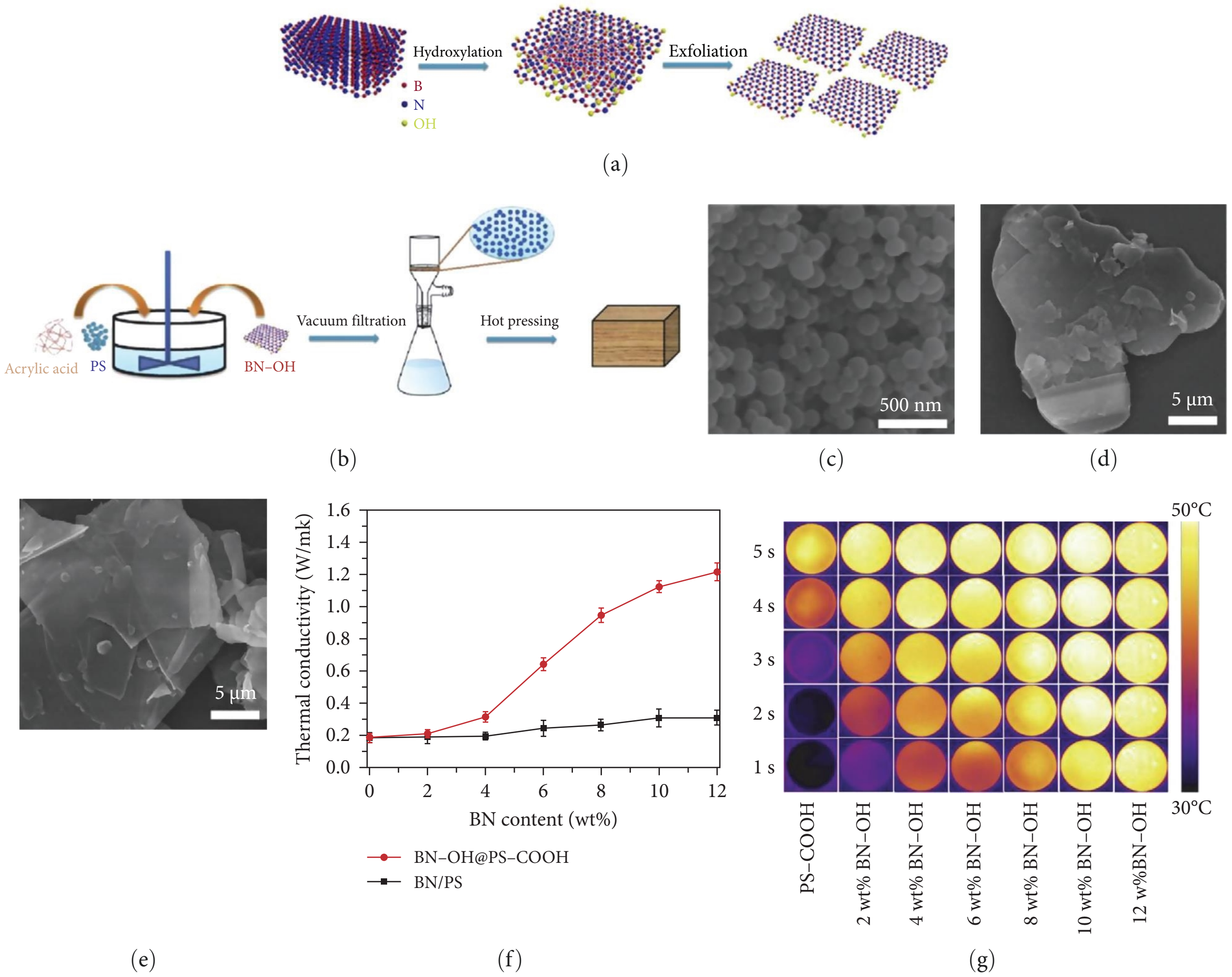

FIGURE 3: Simplified diagram of the preparation of (a) exfoliated BN–OH and (b) BN-based OH/PS–COOH nanocomposites. SEM images of (c) PS–COOH, (d) BN–OH, and (e) 12 wt.% BN-based OH/PS–COOH nanocomposite. Copyright 2016 Elsevier. (f) BN content v/s thermal conductivity and (g) infra-red thermal images of PS–COOH and BN-based OH/PS–COOH nanocomposites [94]. Copyright 2020 Elsevier.

At 6 wt.%, PS–COOH nanospheres are distributed regularly on the BN–OH surface. Figure 3e shows that PS–COOH is tied up with the BN–OH surface; the presence of a large carboxyl group in PS–COOH leads to hydrogen bond formation with a hydroxyl group at the corner of BN–OH and forms stable core–shell structure.

Figure 3f shows the TC of BN/PS and BN-based OH/PS–COOH nanocomposites with different filler loadings. With increasing filler content in BN-based OH/PS–COOH nanocomposite, TC enhanced drastically. The TC of BN-based OH/PS–COOH nanocomposites increased to 1.131 W/m-k with filler loading of 12 wt.% and ~6 times higher than neat/pure PS. Hence, this increases TC due to diffusion of BN–OH filler and good interfacial connection of PS–COOH/BN–OH, which prevent phonon to phonon scattering and promote TC. As presented in Figure 3g, BN–OH@PS–COOH nanocomposites heat up much faster than PS–COOH, with greater sensitivity to BN–OH content. After 5 s, their surface temperature nearly matches that of the hot plate, demonstrating excellent thermal management capability.

3.2. *Orientation of BN Filler.*

Kim et al. [95] claimed that the TC of composite was improved by arranging the anisotropic BN in vertical direction, that is, contingent to heat flow using a magnetic field. BN hexagonal flakes in 2D show anisotropic behavior, for example, having a TC of 600 W/m.K in in-plane, that is ~ 20 times greater than through-plane. The BN coated with iron oxide nanoparticles gets aligned when the magnetic field is applied [95]. The filler weightage should be as low as possible because by increasing the filler amount, degrading the mechanical properties and affects the processing ability of composite. By vertically aligning fillers (BN on which iron oxide is deposited), 30 vol.% of filler loading, thereby, TC was drastically enhanced from 1.765 to 3.445 W/m-k. While depositing iron oxide nanoparticles on BN where BN is pre-coated with polyvinyl pyrrolidone (PVP). Next, iron oxide nanoparticles are deposited, which interact with PVP-coated BN surfaces by electrostatic interaction because of positively charged iron oxide nanoparticles and negatively charged PVP. BN has become a magnetic material after the deposition of iron oxide nanoparticles. BN has severe chemical resistance due to the existence of functional groups on its outer surface. To allow the surface of BN to bond, a surface treatment is required which can be overlooked in recent reports [96, 97]. For more detail, a schematic drawing of BN–Fe_3O_4 synthesis (see Figure 4a).

These particles were then injected into epoxy resin. The epoxy used was bisphenol-A and DDM (4.4′-diamino diphenylmethane) in the ratio of 1:0.4. After preparing epoxy, BN–Fe_3O_4 particles were placed and homogenized, followed by putting in PTFE molds and degassing in the oven for 1 h. The product was placed between two strong magnets (0.4 T) to allow the BN–Fe_3O_4 to align and then cured at 120°C for 3 h. By vertically aligning fillers (BN on which iron oxide is deposited), a drastic increment in TC was observed at 30 vol.% filler loading. Scanning electron microscope micrographs of BN composite with or without magnetic field are displayed in Figure 4b–d [95].

Moreover, Sun et al. [98] prepared composite using polycarbonate (PC) as a matrix and BN plates as reinforcement. The BN plates were oriented using hot-pressing techniques. Proper orientation of reinforcement material builds pathways for TC. This group claimed to increase the TC of 3.09 W/m.K across the orientation with BN volume of 18.5 wt.%.

HoBN/PC showed a TC of 3.09 W/m-K with BN of 18% volume, while the TC of pure PC is 0.2 W/m.K. Figure 4e–g shows a conducting pathway for phonon transport which increases with increasing BN loading continuously. BN was incorporated as reinforcement in the PC matrix, and its percentage continuously increased to analyze the increase in TC. The 18% volume loading shows a sudden positive change in TC, because of providing the easiest path for phonon conduction. Hot pressing incremented the contact area for BN, and thermal contact resistance was diminished accordingly, which eventually offered a reasonable heat transfer rate for in-plane conductivity. Therefore, TC in the through-plane reached 0.86 W/m.K at 18.5 vol.% loading, which is less than in-plane. HoBN/PC is a thermally stable material across the in-plane as its TC increases with the temperature of 30–80°C because phonons can easily cross the barriers between contact of filler and matrix, but with a rise of temperature above 80°C TC decreases due to incense phonon collision. HoBN/PC is a good choice for those electronics applications that need high TC.

Furthermore, it enhanced mechanical properties as BN plates hinder the motion of molecular chains. Storage modulus was increased to 115% for horizontally oriented BN/PC (HoBN/PC) composite with 18.5% volume of BN quantity/loading than pure PC. The preparation of BN/PC composite using the hot-pressing technique a schematic drawing of this process is shown in Figure 4h. The TC of all prepared composites increases continuously with BN loading as shown in Figure 4i. The in-plane TC of HoBN/PC composites rises more rapidly than that of RoBN/PC composites which attributed to contact area between adjacent BN plates in the composite increases, thereby enlarging the effective area for heat conduction and the number of heat conductive pathways when heat is transferred along the BN orientation [99]. Consequently, higher TC and enhancement efficiency are achieved along the orientation through hot pressing. To better illustrate the extent of improvement, the TC enhancement efficiency of aligned BN (ABN) within the matrix is evaluated as the increase in TC per vol% loading. As depicted in Figure 4j, the enhancement efficiency rises with increasing BN content, suggesting stronger interactions between BN plates at higher loadings [100]. Figure 4k presents the heat conduction models of RoBN/PC and HoBN/PC composites, illustrating their distinct thermal conduction mechanisms. In HoBN/PC composites, the improved TC arises from the presence of well-stacked and highly aligned laminated structures, which facilitate more efficient heat transfer compared to RoBN/PC composites.

3.2.1. Characterization of In-Plane and Through-Plane TC.

Comprehending both in-plane and through-plane TC is essential for assessing the material's performance in real world applications based on polymer composites for thermal interface applications [101, 102]. These two types of TC offer valuable insights into how heat is conducted across the material, whether parallel or perpendicular to the composite plane and have a crucial role in the effectiveness of TIMs.

3.2.1.1. In-Plane TC. In-plane TC refers to the ability of the composite material to conduct heat along the plane of the material. In applications where the heat flow is primarily parallel to the surface, such as in flat interfaces or horizontal heat dissipation systems, understanding in-plane conductivity is vital [103, 104]. The alignment direction of filler particles can significantly influence the thermal properties of these materials, specifically the alignment of BN flakes within the composite.

To accurately measure in-plane TC, various experimental techniques can be employed, such as:

- *Laser flash method* (*LFA*): This is widely used technique involves the application of laser pulse to one side of the material. The time it takes for the heat diffusion through the material is measured, allowing for the determination of thermal diffusivity, which can then be used to calculate the in-plane TC. This method is often used for thin materials or when precise measurements of TC are required [105, 106].
- *Hot disk method*: In this method, a sensor is placed between two pieces of material. The installed sensor works as a heat source and thermometer simultaneously to provide a real-time measurements of temperature changes when heat is diffused through the material. By analyzing the temperature rise and heat flux, the in-plane TC can be calculated [107, 108].
- *Steady-state heat flow method*: In this method a heat source is fixed to one end of the material, and the temperature gradient is measured on the opposite side when thermal equilibrium is obtained. By applying Fourier's law of heat conduction, the in-plane conductivity can be determined based on the heat flux and the temperature gradient [109, 110].

In the case of BN-based composites, the in-plane TC is immensely influenced by the orientation of BN flakes. Materials where the BN particles are well-oriented within the matrix tend to have superior in-plane conductivity compared to those

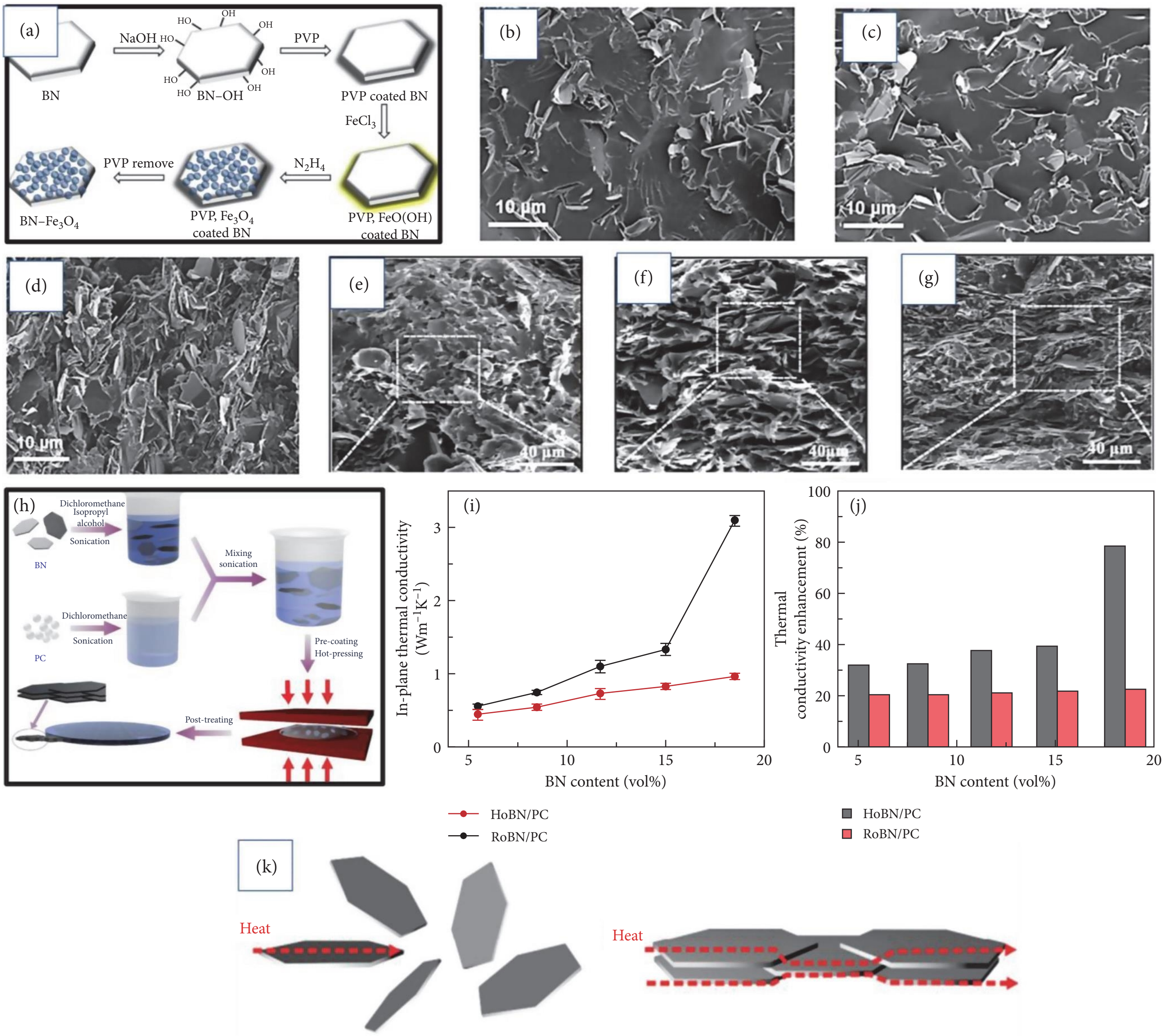

FIGURE 4: (a) Schematic of synthesizing BN–Fe_3O_4. The cross-sectional SEM images of (b) raw BN composite without magnetic field, (c) BN composite with an external magnetic field, and (d) BN–Fe_3O_4 composite with an external magnetic field [95]. Copyright 2016 Elsevier. Microstructure of BN/PC composite taken from SEM (e) Randomly aligned BN/PC composite (11.7 vol.%). (f) Horizontally aligned BN/PC composite (11.7 vol.%). (g) Horizontally aligned BN/PC composite (18.5 vol.%). (h) Schematic diagram of the preparation of HoBN/PC composite by hot pressing. TC of BN/PC composites with different BN quantity/loadings. (i) The in-plane thermal conductivities of HoBN/PC composites, and RoBN/PC composites as a function of BN quantity/loading. (j) The in-plane TC improvement of HoBN/PC composites and RoBN/PC composites in comparison to pure PC. (k) Corresponding heat conduction models [98]. Copyright 2018 Elsevier.

with randomly dispersed fillers. The roll-cutting method, discussed later in the article, performs a central role in achieving this orientation of BN particles, making the composite more effective for thermal management.

3.2.1.2. Through-Plane TC. Through-plane TC refers to the ability of the material to conduct heat perpendicular to the composite plane. In layered or stacked materials, such as in TIMs between electronic chips and heat sinks, the through-plane conductivity is especially significant [45, 111]. The heat flow in these applications generally occurs from the electronic device through the TIM to the heat sink, making the through-plane TC a crucial property.

Several methods can be employed to characterize through-plane TC, such as:

- *Hot plate method*: This method involves applying heat to one side of the material while measuring the temperature on the opposite side. The temperature difference across the material is used to calculate the through-plane TC. It is commonly used for materials with nonuniform thicknesses [107, 112].

- *Guarded hot plate method*: This method is like the hot plate method but with additional thermal insulation around the sample to minimize heat loss. The material's thickness is maintained uniformly, and the temperature gradient through the material is measured accurately, allowing for precise through-plane conductivity values [113, 114].
- *Transient plane source* (*TPS*) *method*: This technique involves placing a tiny sensor between two pieces of the material. The sensor emits heat and measures the time it takes for heat to diffusion through the material, both in-plane and through-plane. This method is particularly useful for measuring TC in anisotropic materials like BN composites, where conductivity differs along different directions [115, 116].

3.2.2. Significance of Directional TC. The anisotropic nature of BN-based composites means that TC is typically not uniform in all directions [117]. In-plane conductivity tends to be higher due to the alignment of BN flakes, whereas through-plane conductivity can be affected by interfacial resistance between layers. Understanding the differences between in-plane and through-plane conductivity is crucial for designing TIMs that are optimized for specific applications [118, 119].

In many interface applications, particularly those involving electronic devices, it is essential to control heat flow in both directions. The roll-cutting method, which helps align BN flakes in the plane of the composite, can improve in-plane TC but may not significantly affect the through-plane conductivity unless specific processing techniques, such as layered stacking or alignment, are employed to address through-plane heat transfer [101, 120].

3.2.3. Linking In-Plane and Through-Plane TC With Applications. For BN-based composites used in thermal interface applications, it is critical to balance in-plane and through-plane conductivity. In cases where the material will be used in vertical heat dissipation (e.g., heat sinks or multilayered packaging), through-plane conductivity becomes more important. On the other hand, for horizontal heat management systems, such as flat interfaces between devices, in-plane conductivity will play a more prominent role [121, 122].

By considering both in-plane and through-plane TC, the BN-based composites can be tailored to suit a variety of applications, ensuring efficient thermal management and heat dissipation. The role of the BN filler orientation, influenced by processing methods like Roll-Cutting, directly impacts the material's thermal performance and should be considered when evaluating its suitability for different thermal interface applications.

3.3. 3D Network Using BN and CNTs. Hu et al. [123] described that the TC of polymer composite increased by creating a 3D path for phonon transport by electrostatic repulsion of positively charged h-BN and linking of silica-coated carbon nanotubes, which claims to enhance the TC up to 1.51 W/m.K which is almost six times greater than neat PVDF. The manufacturing of 3D networks of BN and CNT provides good mechanical and insulation properties as well. PVDF is an excellent candidate for electronic assemblies for its facile fabrication, better mechanical properties, thermal stability, and electrical insulation [124]. The neat PVDF possesses a TC of ~ 0.22 W/m.K, which hinders its usage in practical applications. The heat transfer rate increases by reinforcing it with various fillers with intensive loadings [125, 126], which makes the product expensive, so the task is to attain a high TC at minor filler quantity/volume. Enhancing the TC of composite by creating a 3D network is a new area of research [127]. CVD [128], hydrothermal method [129], and bidirectional freezing technique [130] are the most common techniques. These techniques can increase TC at a certain level with addition of filler content.

Hu et al. [123] reported that a thermally conductive 3D network was constructed in PVDF matrix by the electrostatic repulsion of positively charged hBN (m-hBN) and linking MWCNT-SiO_2. The preparation of 3D network composite starts with modification of hBN which is depicted schematically in Figure 5a–c. To improve the ability of heat dissipation, the synthesis patterns/level of 3D networks in PVDF material/composite has been shown in Figure 5d, e. The 3D networks are established by the combined effect of m-hBN and MWCNTs-SiO_2. The thin and elongated MWCNT–SiO_2 hybrids served as connections between the well-dispersed m-hBN platelets, facilitating the movement of phonon.

Figure 5f demonstrates the capability m-hBN and MWCNTs-SiO_2 for making 3D networks. The thin and elongated MWCNTs-SiO_2 hybrids are dispersed between adjoining m-hBN platelets, effectively connecting them, and facilitating the development of thermally conductive pathways. The morphological study of m-hBN and MWCNTs-SiO_2 surfaces was examined by TEM. However, a uniform and thin amorphous layer of 3.58 nm was coated on hBN (see Figure 5g).

Figure 5h illustrates the TC and enhancement of PVDF composites with respect to pristine/pure PVDF matrix. A gradual increase has been seen in TC with increasing filler loading up to 25 wt.%, indicating a vital role of fillers in facilitating heat conduction. Notably, the m-hBN/PVDF composite exhibits higher TC compared to hBN/PVDF even with identical filler loadings, which attributed to better solubility/mixing and stronger interfacial bonding of m-hBN. These factors likely contribute to reduced phonon scattering at the filler/matrix interface. Likewise, the m-hBN/MWCNTs-SiO_2/PVDF composite having a 25 wt.% filler loading attains a maximum TC of 1.51 W/m·K, representing an enhancement of ~5.86 times superior to pristine/pure PVDF. However, a degradation in TC is observed beyond 25 wt.% filler loading, merely ascribed to aggregation of filler within the polymer matrix, strengthens the phonon scattering and hinders the thermal transport [131]. To explore TC enhancement of m-hBN/MWCNTs-SiO_2/PVDF composites an effective medium approximation (EMA) model was applied as shown in Figure 5i. The data of Figure 5i elucidates the ITR of hBN/PVDF and m-hBN/PVDF which deteriorated 43.9% due to the co-modification of PDA and APTMS. Besides, the ITR of m-hBN/MWCNTs-SiO_2/PVDF was further decreased after incorporating MWCNTs-SiO_2. Hence, the predicted results of EMA model employ that

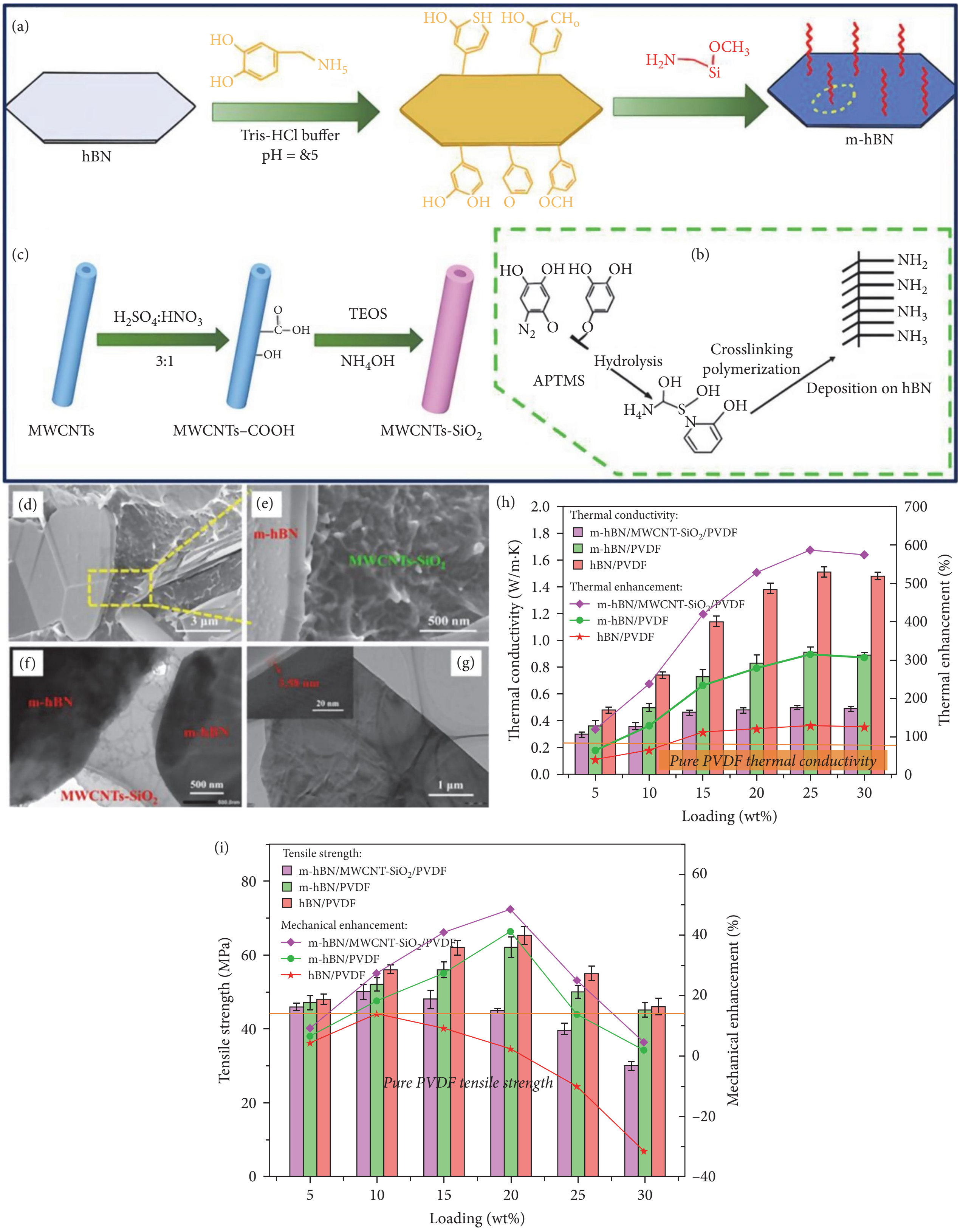

FIGURE 5: Schematic drawing of (a) the procedure of m-hBN synthesis, (b) the potential reaction mechanism of m-hBN, (c) the synthesis process of MWCNTs-SiO$_2$. (d) and (e) Cross-sectional SEM images of PVDF composites with the loading of 15 wt.% m-hBN/MWCNTs-SiO$_2$. TEM image of (f) the connected m-hBN with the bridging of MWCNTs-SiO$_2$ (mass ratio: 4:1) and (g) m-hBN. (h) Thermal conductivity. (i) Tensile strength of PVDF composites with different filler volume/loadings [123]. Copyright 2020 Elsevier.

the surface modification of hBN and formation of 3D-networks have synergic effect for lowering the resistance of interfacial thermal.

Chen et al. [132] studied the enhancement of TC in epoxy nanocomposite up to 1400% with 9.6 vol.% BNNSs as filler. Chen et al. used cellulose nanofibers that supported 3D interlinked BNNSs. They used sol–gel and freeze–drying techniques to design a 3D BNNS network, where BNNSs self-assembled on a 3D cellulose skeleton applying the techniques mentioned above. After preparing 3D BNNSs aerogel, epoxy resin penetrated 3D BNNSs aerogel, which ultimately formed a high thermally conductive composite. With 9.6 vol.% of filler loading, the TC of 3.13 W/m-k was attained, which refers to improved TC of almost 1400%. Filler loading can vary the thermal conducting properties; this composite is electrically insulator, which makes it a promising candidate for thermal management, for example, electronic packaging, electrical insulation, etc. Thermal conducting networks enhance the TTE per unit filler mass. It is considered that the TC of BNNSs relies on multiple sheets. Other, Jo et al. [133] asserted that BN comprising 11 layers of nanosheets exhibits a TC of 360 W/m-k, approximately equal to TC of basal plane of h-BN. The TC of the composite has been enhanced promisingly with few layers of BNNSs.

Chen et al. [132] followed the synthesis rout of epoxy/3D-C-BNNS nanocomposites as shown in Figure 6a. Initially, they started with the dissolution of cellulose in NaOH/urea liquid solution. After that, BNNSs were put on to prepare cellulose/BNNS collosols. In this collosol, cellulose worked as a stabilizing element for BNNSs. Because of the hydrolysis reaction in the sonication process, hydroxyl groups and amino groups were located on the boundaries/edges of exfoliated BNNSs [99]. So, hydrogen bonding can be bridged between BNNSs and the cellulose skeleton, leading to the absorption of BNNSs in the cellulose skeleton. Cellulose nanofibers worked as a bridge to join BNNSs. The epichlorohydrin served as a crosslinking agent of cellulose to build 3D-C-BNNS hydrogel. If cellulose and BNNS mixtures sustained stable colloidal dispersion before crosslinking, they could attain porous aerogel further frozen in liquid nitrogen. At liquid nitrogen temperature, hydrogen suddenly becomes solid and does not let the crystals grow and shatter the 3D-C-BNNS skeleton; this freezing process results in a building frame-like structure [134, 135]. The resulting aerogel kept the form of 3D-C-BNNSs; epoxy was injected through the vacuum to get epoxy/3D-C-BNNSs nanocomposite.

The prepared composite (cellulose aerogel, 3D-C-BNNS$_{12}$ aerogel, 3D-C-BNNS$_{24}$ aerogel, and BNNSs) were centrifuged, collected, and their microstructures were analyzed using SEM and TEM as shown in Figure 6b–h. These outcomes revealed that the h-BN obtained by exfoliation consists of thin and rolled nanosheets. By Figure 6g, it is evident that BNNSs are foldable and show plastic behavior. The BNNSs are peeled/exfoliated from bulk BN, through the electron diffraction pattern of exfoliated BNNSs, it is seen that exfoliated BNNSs also have a hexagonal structure. In addition, the statistical data of atomic force microscopy (AFM) images of BNNSs (see Figure 6 i,j), confirmed that the average thickness of BNNSs is 2–3 nm and the lateral size is 1–2 μm.

Figure 6k,l shows the TC of nanocomposite with different filler quantity/loading and temperature. Figure 6k shows the increment of TC up to 3.13 W/m.K with 9.6 vol.% filler loading at ambient conditions, which is ~16 times more than neat epoxy and 11 times more than nanocomposite with randomly distributed BNNSs. It is worth noticing that the TC graph grows linearly with BNNS concentration. A higher amount of BNNSs creates a thermal conductive network and increases TC. Figure 6I demonstrates the temperature dependent TC of the epoxy resin, epoxy/3D-C, epoxy/BNNS, and epoxy/3D-C-BNNS. The thermal conductivities of these composites are vaguely increases when temperature increases from 25 to 125°C but in epoxy/3D-C-BNNS nanocomposites, the TC increases comparatively fast with temperature. The TC of epoxy/3D-C-BNNSs reaches up to 4.04 W/m.K at 125°C, which is 29% higher as of at room temperature. This improvement is possibly due to large thermal expansion coefficient of epoxy resin.

3.4. Roll-Cutting Processing Method. Yin et al. [136] prepared a silicon rubber and ABN composite, and two different processes were employed to prepare the composite, that is, stack cutting and roll cutting. The ABN composite prepared by a roll-cutting method shows good TC than the stack-cutting method [136].

Two techniques were applied to prepare the composites are follows: first, silicon rubber (MVQ) and BN composites were made by mixing MVQ, BN, and 2,5-dimethyl-2,5-di (tert-butyl peroxy) hexane (DBPMH) in two-roll mill whereas an optimized addition of BN content and appropriate blending time is required to get uniform dispersion of BN in the matrix. Further, to prepared MVQ/ABN composites two different methods have been adopted. First is the stack cutting method in which a batch of MQV/BN composite, by using a hydraulic press, undergoes a compression at 25°C for 1 min to get 0.5 mm thick films. This film was cut down in rectangular form having a size of 100 × 50 mm, and 100 × 2 mm, thereby, stacked to form MVQ/ABN compounds of 2 mm thickness, as shown in Figure 7a. Subsequently, MVQ/ABN stack was cured in a mold by using hydraulic hot press at the temperature of 170°C under 8 MPa pressure for 20 min to prepare the first composite (MVQ/ABN-I).

The second method was used to prepare a composite of MVQ/ABN which subsequently undergoes compression by hydraulic press to tightly rolled for the cylindrical form of ~ 10 mm diameter. This was further cut to get slices of 2 mm thickness by cutting in the normal direction to the axis, as shown in the Figure 7b. Finally, these slices were also cured at 170°C for 20 min in the hot oven to achieve the MVQ/ABN-II composites.

However, results revealed that MVQ/BN composite prepared by roll cutting method provided the PC of 6.341 W/m.K, while the composite accomplished by stack cutting method showed a TC of 5.972 W/m.K, which inferred that the cutting method can significantly create the thermal conductive pathways by appropriate induction of BN flakes in composite [136].

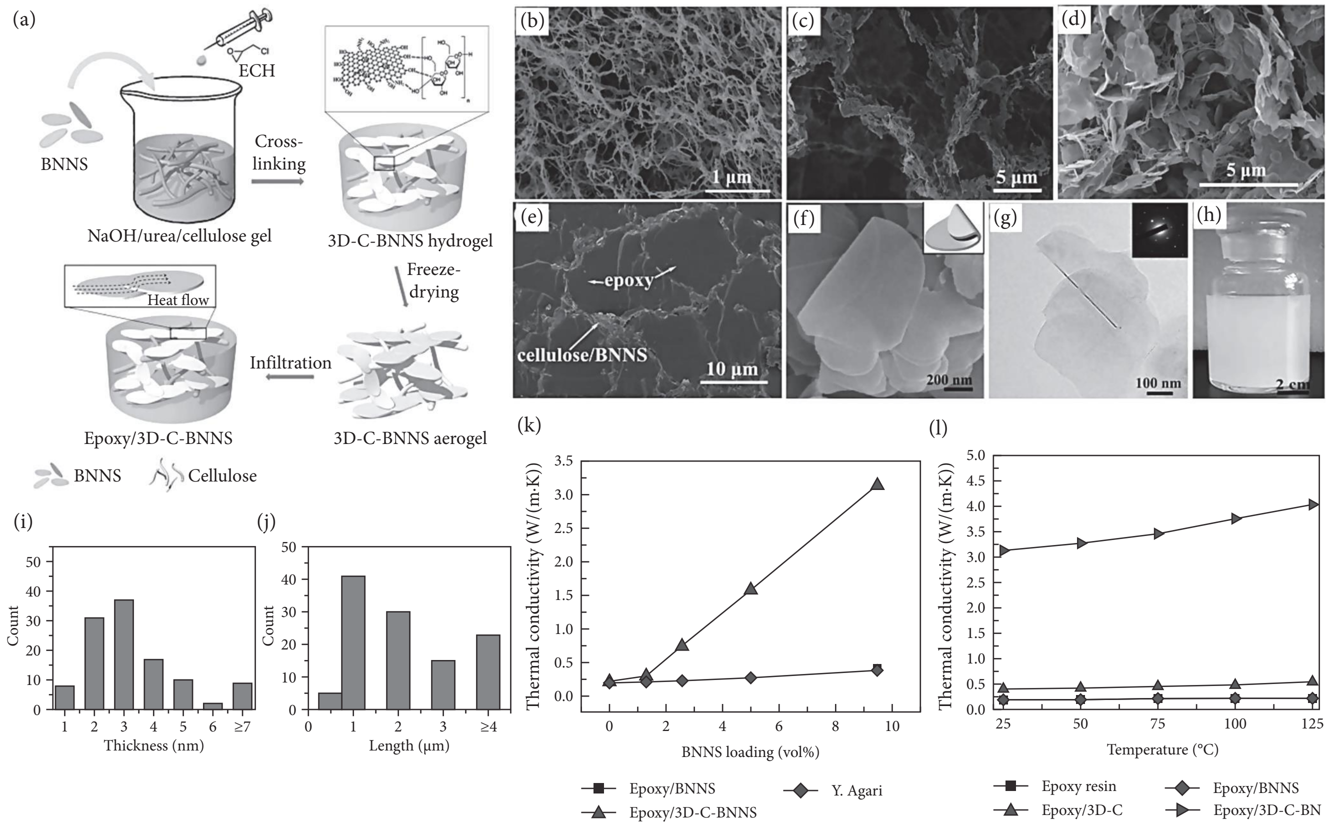

Figure 6: (a) Simplified diagram of synthesis process of epoxy/3D-C-BNNS nanocomposites. SEM images of (b) cellulose aerogel, (c) 3D-C-$BNNS_{12}$ aerogel, (d) 3D-C-$BNNS_{24}$ aerogel, (e) SEM images of fractured surface of epoxy/3D-C-$BNNS_{24}$ nanocomposite. (f) SEM, (g) TEM image of BNNSs, (h) photograph of exfoliated BNNS supernatant, (i) thickness, and (j) statistical analysis results of BNNSs according to AFM topographic images, (k) TC at room temperature, and (l) Temperature dependent TC of epoxy/BNNS nanocomposites [132]. Copyright 2017 Wiley.

The SEM study was established to examine the surface and fracture morphologies of the MVQ/BN and MVQ/ABN composites. Figure 7c–e represents the SEM images of MVQ/BN_{d30}-80, MVQ/ABN_{d30}-80-I, MVQ/ABN_{d30}-80-II. Here, d30 shows the average particle's diameter, and 80 indicates the percentage content whereas I and II are techniques (I, stack-cutting method and II, roll-cutting method).

The SEM analysis clearly depicts the orientation of BN in MVQ/ABN_{d30}-80-I and MVQ/ABN_{d30}-80-II as compared to MVQ/BN_{d30}-80 composite. Hence, BN as 2D filler invokes in-plane orientation alignment under compression [137].

However, the TC of ABN composites is higher than non-ABN composites, and average particle size significantly impacts TC as 30-micrometer particle size has higher TC than 10 micrometers. The TC of pure silicone rubber (SiR) is just 0.2 W/m.K, which is enhanced to ~ 6 W/m.K by reinforcing BN and processing through the roll-cutting method [136].

The roll-cutting processing method results in the alignment of BN particles within the composite, an essential factor for improving the material's TC. The alignment of BN flakes through this method encourages the creation of efficient thermal conductive routes. This is significant because the orientation of the BN 2D filler has a profound impact on the absolute performance of composite. Particularly, the ABN particles facilitate the flow of heat more effectively than randomly distributed ones, resulting in enhanced TC.

The role of filler orientation in composite materials is well-established, and the ABN flakes contribute to more effective heat conduction by establishing continuous directional thermal pathways. This is because the aligned particles create a structured network that supports heat transfer in a more organized and effective manner [138–140].

The alignment of BN flakes through this method results in anisotropic TC, where the composite exhibits different thermal conductivities along different directions, which is a characteristic of oriented fillers. While the roll-cutting method is an essential technique for producing SiR/BN composites, its impact on the orientation of BN fillers is central to the material's thermal performance [141].

3.5. Covalent Coupling of BN With Other Polymer Matrices.

BN is composed of boron–nitrogen covalent bonds which usually used as a refractory material. In covalent bonding, atoms share their valence electrons to form a strong chemical bond. The BN generally makes weak bonding with other polymer materials due to its inert and unreactive surface, enabling it complicated to form strong chemical interactions [142]. Since, the covalent bonding of BN filler with other polymer matrices

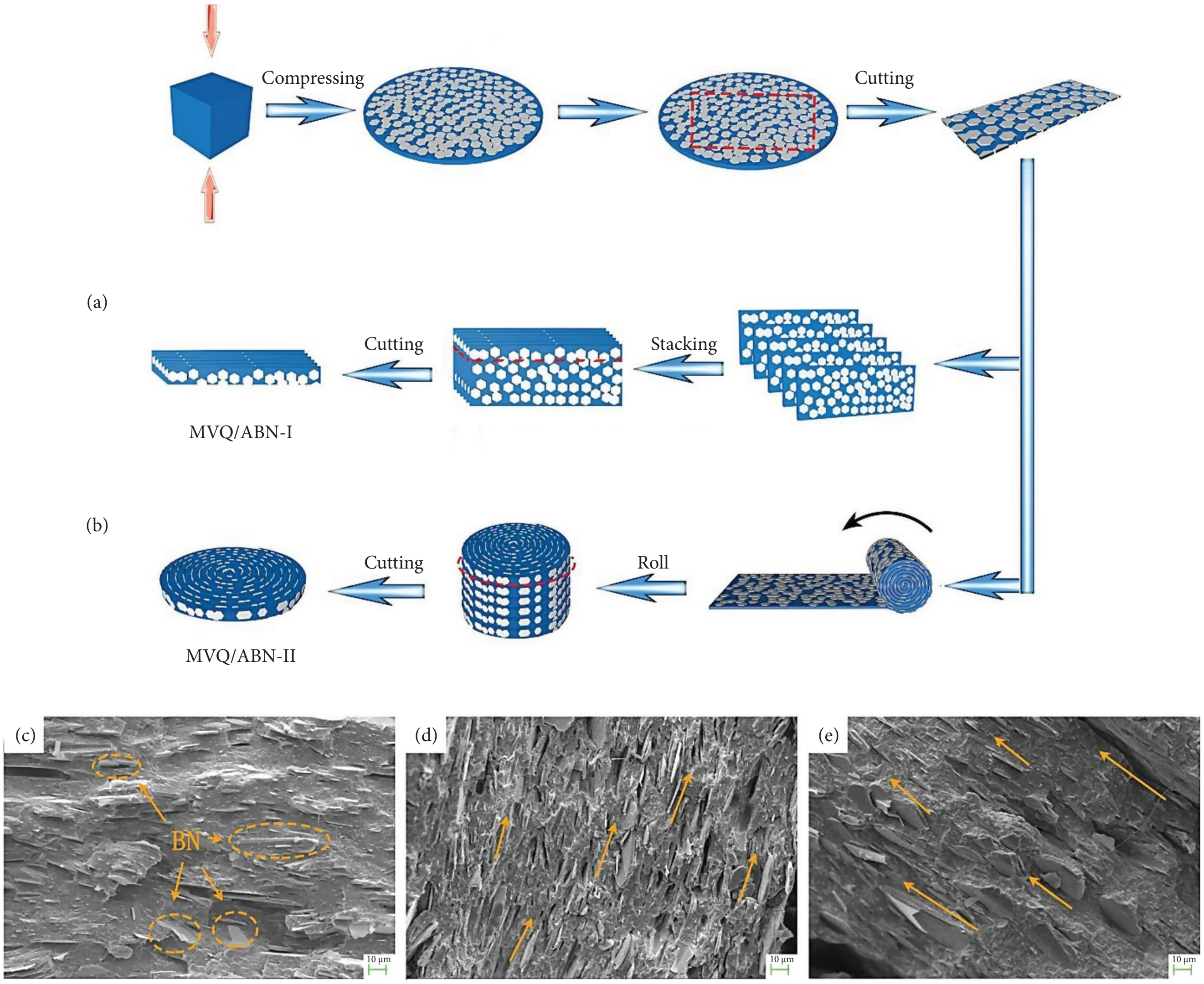

Figure 7: (a) Silicone rubber/BN composite by stack cutting method, (b) silicone rubber/BN composite by roll cutting method. SEM images of (c) MVQ/BN$_{d30}$-80, (d) MVQ/ABN$_{d30}$-80-I, and (e) MVQ/ABN$_{d30}$-80-II [136]. Copyright 2021 Elsevier.

(epoxy resins, PS, natural rubber, etc.) commonly two methods are implemented, that is, introduction of functional groups and surface modification of BN. To form covalent bonds with other polymer matrices, BN is being functionalized with reactive groups like azide (–N$_3$) and silanes [143, 144]. The strong covalent bonding of BN with different polymer matrices improves the dispersion of the BN fillers in matrix and interfacial interactions, which ultimately enhance the compatibility, mechanical properties, and TC [142, 145, 146].

For example, in 2020 Cheng et al. [147] claimed to enhance the TC of composite by building covalent bonds between filler and matrix. This group introduced different silane coupling agents (SCAs) bonding polyvinyl alcohol (PVA) and functionalized BN (fBN) to systematically investigate the TC of PVA–fBN composite. Cheng et al. added the SCAs and observed their impact on the TC of the composite. It was observed that a SCA with a short side chain, that is, vinyl triethoxysilane, has enhanced the TC of the composite to 1.636 W/m.K, which is ~337.3% of PVA–fBN [147]. With the addition of BNNS fillers in the PVA matrix, the TC of the composite is enhanced to 18.63 W/m.K in-plane by creating hydrogen bonding between filler and matrix through hot-pressing technology [148]. The TC of the composite increased by developing van der Walls forces between BN and PS based on emulsion template [149]. Noncovalent bonding between filler and matrix reduces the scattering of phonons and decreases ITR [150]. Making covalent bond between filler and polymer matrix to enhance TC is a suitable mechanism [151]. SCAs are used in many experiments to increase TC. Moreover, low-concentration SCAs increase TC, while high concentrations diminish it [151].

3.6. Role of BN Orientation. Zhang et al. [152] investigated the thermal transport properties of binary filler-based SiR composites by examining the spatial distribution effects of hybrid fillers. Unlike prior reports that focusing on size of filler, shape, structure, and constitutes, this report emphasizes the influence of filler orientation on TC. Here, they proposed a binary-filler strategy using anisotropic 2D h-BN and isotropic 0D spherical alumina (S–Al_2O_3). The h-BN filler is aligned to maximize its intrinsic TC properties, while the S–Al_2O_3 particles are strategically positioned between adjacent h-BN layers. This arrangement significantly enhances the through-plane (2.132 W/m·K) and in-plane (14.581 W/m·K) TC values of the SiR composites (40 vol.% h-BN and 5 vol.% S–Al_2O_3). In another study, Liang et al. [153] explored the enhancement of TC in epoxy resin composites by incorporating h-BN through AC electric field induction. Where epoxy resin is extensively used in microelectronic packaging due to its excellent electrical insulation, mechanical properties, and low TC (0.14 W/m·K), limits its application in high-power components. To overcome this limitation, they developed h-BN/EP composites with a small filler quantity/loading (10 wt.%) while achieving high TC. By applying an AC electric field of 120 V/mm at 50 Hz for 1 h, they attained a TC of 0.310 W/(m·K), 2.214 times higher than pristine/pure epoxy resin and 1.325 times higher than conventional h-BN/epoxy resin composites without orientation control.

Niu et al. [154] focused on the development of high-performance TIMs with high through-plane TC, softness, and electrical insulation, which are essential for modern electronics but to achieve all these properties simultaneously is a challenge. To compete the issues, authors used the stacking-cutting method to fabricate BN film-filled SiR composites. It preserved the high orientation of BN films, resulting in a record-high through-plane TC of ~ 19.1 W/m·K while maintaining a low compressive modulus of 5.42 MPa, ensuring softness and flexibility. The low BN content (37 vol.%) further enhances the strength of material.

By employing an advanced interface engineering strategy, Zhou et al. [155] explored the development of flexible polyamide-imide (PAI) thermally conductive composite films and addressed the challenge of phonon transmission discontinuity, which hinders TC in composite materials. They used a layer-by-layer construction approach to make a hierarchical structure comprising fBN and polydopamine-modified BNNTs. They noted that the optimized hybrid filler structure significantly improves phonon transmission, reducing scattering and enhancing heat transfer efficiency and the composite film achieves an ultrahigh TC of 71.1 W/m·K, marking a 3663% enhancement compared to traditional polymer materials.

For more detailed insights, Table 1 provides an overview of enhancing thermal study of different polymer composites based on BN, prepared through various techniques. In this table, we summarized the TC values of several BN/polymers composites to comprehend the performance of BN as filler.

4. Thermal Interface Applications Based on BNNSs

BNNSs have gained significant attention as TIM having their excellent TC and electrical insulating properties. The diversity of fabrication techniques has been established for synthesizing BNNSs, where the thermal performance is largely modulated by its thickness, lateral dimensions, and quantity [121]. Therefore, when BNNSs are incorporated into different polymer matrices, TC is promising enhanced and infer an efficient heat dissipation for modern applications [101].

For example, Jiang et al. [157] reported a stretchable and self-healable TIM based on BNNSs and a dual-cross-linked hydrogel. This can boost the thermal transfer and recover from damage, possibly advancing heat dissipation materials. Similarly, Zhan et al. [102] presented an interfacial arc-like phonon bridge approach to mitigate the thermal contact resistance in BNNS-based composites. This strategy could be used for cooling in fast-charging batteries at industrial level. Moreover, in another study researchers developed a vertically aligned BNNSs films (VBNFs) using a microfluidic spinning process and template-assisted CVD conversion method [158]. The VBNFs are applied as fillers to make TIMs and attained high TC (6.4 W/m.K) and low modulus (2.2 MPa at low BN loading), contributing high cooling performance for thermal management high-power electronics. Hence, these advancements in BNNS-based TIMs provide remarkable solutions for thermal management challenges in recent complex electronics devices.

5. Prospects

BN and its derivatives hold significant promise for next-generation technologies owing to their exceptional TC, chemical stability, electrical insulation, and mechanical robustness. The combination of high in-plane phonon transport and wide bandgap characteristics enables their integration into a wide range of emerging applications as depicted in Figure 8. Looking ahead, several key prospects are highlighted:

5.1. Electronic Appliances. The BN nanostructures including, nanotubes, nanoparticles, and nanosheets, exhibit a range of emerging properties of high TC, excellent electrical insulation, better resistance to corrosion and oxidation, chemical inertness, biocompatibility, hydrophobicity, lubricity, and outstanding mechanical strength. Due to their exceptional TC-, BN- and BN-based polymer composites are appropriate to use in electronic circuit assemblies to eradicate the heat generated in components such as CPU processors, mobile phones, and motherboards. Additionally, the ceramic nature of BN makes it a suitable fire-retardant material for electrical switches, particularly under short-circuit conditions. In electric motors, which works for long period of time and produce considerable heat, but BN-based coatings can be applied to the body of motor to enhance heat dissipation and improve both operational integrity and durability.

5.2. Vehicles. The disc brakes have central role in the braking systems of vehicles, where the contact between the brake pad and disc generates large amount of frictional heat. However, the incorporation of BN into the pad material can circumvent the heat accumulation due to TC of BN. Nevertheless, the BN-based polymer coatings further support by providing TC and excellent resistance to corrosion and oxidation.

Moreover, when BN is mixed in engine oils, it works for both enhancing heat transfer and providing effective lubrication to critical engine components such as piston rings, pistons, and cylinder walls. These advantages jointly improve the

Table 1: Overview of enhanced TC of polymer by addition of BN.

Polymer	**Filler and loading**	**Technique**	**Thermal conductivity (W $m^{-1}K^{-1}$)**	**References**
PDMS	15 wt.%SCF/20%BN	Spin coating	2.29	[93]
Epoxy (Bisphenol-A& DDM)	30% BN–Fe_3O_4	Aligned under magnetic field	3.445	[156]
Polycarbonate	18.5 vol.% BN plates	Hot pressing	3.09	[98]
BN–OH@PS–COOH	12 wt.% addition of BN–OH	Nanocomposite	1.131	[94]
PVA	fBN, Silane coupling agent	Electro-spinning and hot-pressing	1.636	[147]
Silicone rubber	54 vol.% Hexagonal BN	Hydraulic press compression	6.341	[136]
Epoxy	BNNS 20 vol.%	Bidirectional freezing	6.54	[130]
PVDF	h-BN silica-coated CNT (25% filler)	Solvent-casting	1.51	[123]
Epoxy resin	Sol–gel	Sol–gel freeze–drying	3.13	[132]

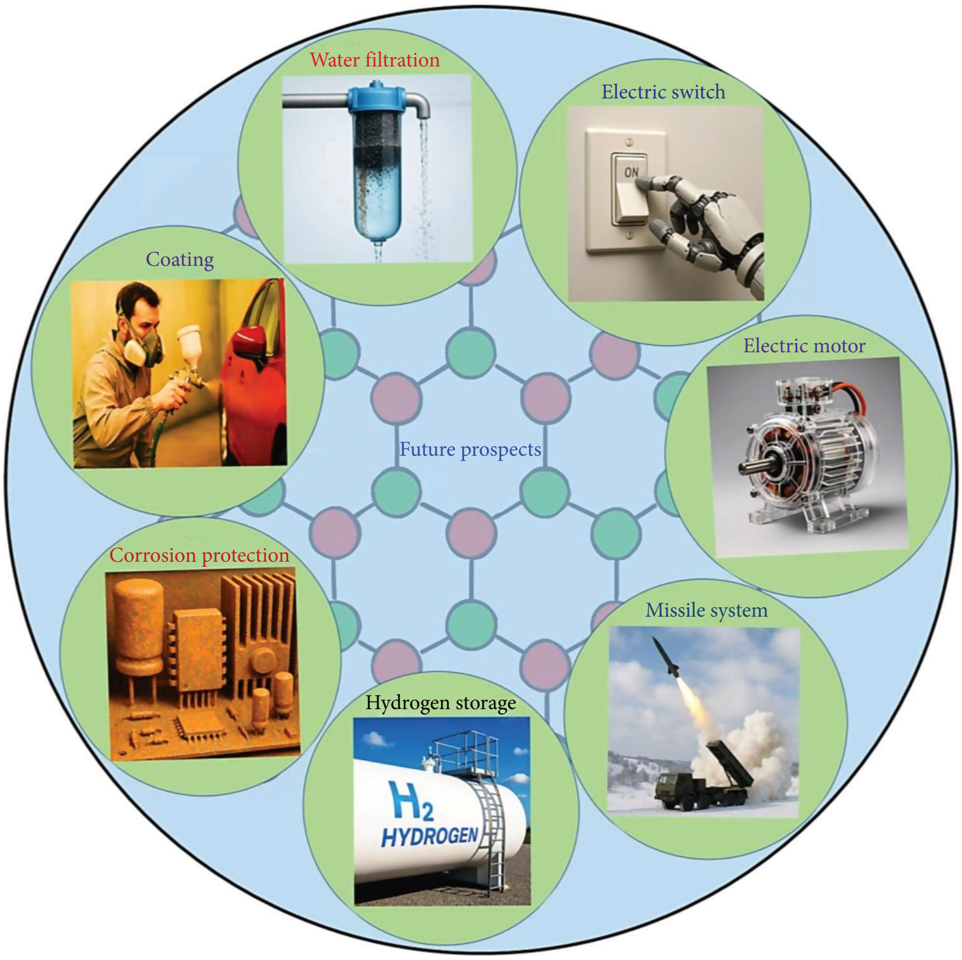

Figure 8: Prospects of BN-related materials for next-generation technology.

efficiency and extend the operational lifetime of combustion engines.

5.3. Hydrogen Gas Storage and Water Purification. The BN has several advantages owing its compact nanostructure, such as storing hydrogen gas. Generally hydrogen gas can be escaped from interstitial vacancies of conventional steel tanks, but interestingly the polymeric composites can prevent hydrogen from escaping [159, 160]. Another potential application of BN, owing to its nanostructured configuration, is in the filtration of effluent gases. Some gas components can be successfully captured within the BN nanostructure, thereby enabling the purification of the gasses.

Also, the contaminated water can be filtered by BN because of its properties of hydrophobicity, BN can dissolve organic solvents and oils, leaving the clean water behind and further the BN can be quickly recharged for reuse by heating it at high temperatures and removing the detained solvents. The intrinsically hydrophobicity, BN can be utilized as a filler in surface coatings for automotive exteriors and low-pressure gas pipelines, which effectively deicing and improving the operational reliability in winter season.

5.4. Missile and Defense Systems Technology. The BN, especially in its h-BN and nanoscale forms (e.g., BNNTs and BNNSs), extends the promising scope for advanced thermal management in missile and defense systems technology due to its auspicious traits of properties. There is various perspective on its future applications of missile and defense technologies:

- Due to high TC the electrical insulation can protect sensitive missile components from overheating.
- The stability of BN in extreme environments like high radiation can support the space-based missile systems.
- Excellent TC of BN renders the high-power RF and radar components in aerospace and defense technology.
- The BN-based TIMs could be the game changer for next-generation strategic missile defense implications.

6. Conclusion

In summary, this review provides a comprehensive overview of BN-based polymer composites with high TC for thermal interface applications. We have outlined key advances in BN synthesis, thermal characterization, its role as a composite filler, and the benefits of covalent coupling. It is concluded that BN fillers create continuous thermal conduction pathways, facilitating phonon transport and significantly influencing the overall TC of composites. While TC is generally higher in parallel alignment than in perpendicular orientation, increasing filler content consistently enhances TC. Moreover, hot-pressing techniques can directionally align fillers, further promoting phonon movement.

However, these factors embark the emerging properties of BN materials in enhancing thermal management, mechanical strength, chemical resistance, and interfacial bonding within composites. Furthermore, we demonstrated several limitations and prospect applications of structural change at very high temperatures, thermal degradation, sintering challenges, thermal shock resistance and scalability that need to be addressed in future for next-generation technology. The implications of our review are far-reaching, signifying an efficient utilization in assemblies of electronic devices, 5G telecommunication technology, slim LED TVs, super processor cell phones, and fast charging of heavy charge storing batteries.

However, our review study offers a general strategy for designing advanced thermal management materials for wearable and intelligent electronic equipment.

Data Availability Statement

The data can be provided on special request to the corresponding author.

Conflicts of Interest

The authors declare no conflicts of interest.

Author Contributions

Muneeb Ur Rehman and Muhammad Faheem Maqsood contributed equally.

Funding

This project is funded by the NRF Korea ICT basic research program (Grant 2022R1F1A1075229). The authors extend their appreciation to the Deanship of Research and Graduate Studies at King Khalid University, Saudi Arabia, through Large Research Project under Grant RGP-2/695/46.

Acknowledgments

We are very grateful to Henan University, China and American University of Sharjah, United Arab Emirates to support this study.

References

[1] W.-L. Song, W. Wang, and L. Monica Veca, "Polymer /Carbon Nanocomposites for Enhanced Thermal Transport Properties-Carbon Nanotubes Versus Graphene Sheets as Nanoscale Fillers," *Journal of Materials Chemistry* 22, no. 33 (2012): 17133–17139.

[2] M. Abubakr, E. Elahi, S. Rehman, et al., "Innovations in Self-Powered Nano-Photonics of Emerging and Flexible Two-Dimensional Materials," *Materials Today Physics* 39 (2023): 101285.

[3] E. Elahi, S. V. P. Vattikuti, M. Ahmad, et al., "Extant Developments in Two-Dimensional Materials and Their Integration for Sensing Applications in Innovative Era," *Materials Today Chemistry* 48 (2025): 102886.

[4] L. P. Maiorano, M. Guidoum, and J. M. Molina, "Low-Porosity Aluminum Foams With Steel Guest Phases as Disruptive Materials for Active Thermal Management," *Applied Materials Today* 42 (2025): 102530.

[5] Y. Lin, Q. Kang, Y. Liu, et al., "Flexible, Highly Thermally Conductive and Electrically Insulating Phase Change Materials for Advanced Thermal Management of 5G Base Stations and Thermoelectric Generators," *Nano-Micro Letters* 15, no. 1 (2023): 31.

[6] Y. Chen, H. Zhang, J. Chen, et al., "Thermally Conductive But Electrically Insulating Polybenzazole Nanofiber/Boron Nitride Nanosheets Nanocomposite Paper for Heat Dissipation of 5G Base Stations and Transformers," *ACS Nano* 16, no. 9 (2022): 14323–14333.

[7] Z. Han and A. Fina, "Thermal Conductivity of Carbon Nanotubes and Their Polymer Nanocomposites: A Review," *Progress in Polymer Science* 36, no. 7 (2011): 914–944.

[8] M. Grujicic, C. L. Zhao, and E. C. Dusel, "The Effect of Thermal Contact Resistance on Heat Management in the Electronic Packaging," *Applied Surface Science* 246, no. 1–3 (2005): 290–302.

[9] Y. Guo, K. Ruan, X. Shi, X. Yang, and J. Gu, "Factors Affecting Thermal Conductivities of the Polymers and Polymer Composites: A Review," *Composites Science and Technology* 193 (2020): 108134.

[10] X. Li, J. Lin, J. Wu, et al., "Stretchable and Leakage-Free Liquid Metal Networks for Thermal Management," *Advanced Functional Materials, n/a (n/a)*: 2420839.

[11] J. Tan and Y. Zhang, "Thermal Conductive Polymer Composites: Recent Progress and Applications," *Molecules* 29, no. 15 (2024): 3572.

[12] Y. Guo, Y. Zhou, and Y. Xu, "Engineering Polymers With Metal-Like Thermal Conductivity—Present Status and Future Perspectives," *Polymer* 233 (2021): 124168.

[13] S. Zhu, S. Wu, Y. Fu, and S. Guo, "Prediction of Particle-Reinforced Composite Material Properties Based on an Improved Halpin–Tsai Model," *AIP Advances* 14, no. 4 (2024): 045339.

[14] Z. Jiang, G. He, Y. Duan, et al., "Contrasting Effects of Various Factors Upon the Properties of Foam Ceramics and the Mechanisms of Crystalline Phase Reconstruction and Microstructure Regulation," *Ceramics International* 50, no. 12 (2024): 21645–21657.

[15] E.-C. Cho, J.-H. Huang, C.-P. Li, et al., "Graphene-Based Thermoplastic Composites and Their Application for LED Thermal Management," *Carbon* 102 (2016): 66–73.

[16] A. L. Moore and L. Shi, "Emerging Challenges and Materials for Thermal Management of Electronics," *Materials Today* 17, no. 4 (2014): 163–174.

[17] A. Wazeer, A. Das, C. Abeykoon, A. Sinha, and A. Karmakar, "Phase Change Materials for Battery Thermal Management of Electric and Hybrid Vehicles: A Review," *Energy Nexus* 7 (2022): 100131.

[18] P. Kumar, D. Chaudhary, P. Varshney, U. Varshney, S. M. Yahya, and Y. Rafat, "Critical Review on Battery Thermal Management and Role of Nanomaterial in Heat Transfer Enhancement for Electrical Vehicle Application," *Journal of Energy Storage* 32 (2020): 102003.

[19] A. Aryanfar, F. Elias, and W. A. Goddard III, "Enhancing the Thermal Dissipation in Batteries Via Inclusion of Central

Heat Sink," *Journal of Electrochemical Energy Conversion and Storage* 21 (2023): 021003.

[20] M. Ge, Q. Li, J. Zhang, et al., "Enhancing Thermal Conductivity of the Insulating Layer of High-Frequency Copper Clad Laminates Via Incorporating Surface Modified Spherical hBN Fillers," *Journal of Materials Science: Materials in Electronics* 31, no. 5 (2020): 4214–4223.

[21] Y. Zhang, Z. Geng, S. Niu, S. Zhang, J. Luan, and G. Wang, "Preparation and Applications of Low-Dielectric Constant Poly Aryl Ether," *Advanced Industrial and Engineering Polymer Research* 3, no. 4 (2020): 175–185.

[22] M. Sattanathan, S. Subramani, K. Mohamed, M. Devarajan, and R. M. Nasir, "Synthesis and Characterization of Hexagonal Boron Nitride Coating on Polyethylene Terephthalate," *Iranian Polymer Journal* 28, no. 11 (2019): 969–976.

[23] S. M. Z. Mehdi, M. F. Maqsood, A. Dahshan, et al., "Emerging Boron Nitride Nanosheets: A Review on Synthesis, Corrosion Resistance Coatings, and Their Impacts on the Environment and Health," *Reviews on Advanced Materials Science* 63, no. 1 (2024).

[24] S. Pandit, K. Gaska, V. R. S. S. Mokkapati, et al., "Antibacterial Effect of Boron Nitride Flakes With Controlled Orientation in Polymer Composites," *RSC Advances* 9, no. 57 (2019): 33454–33459.

[25] P. V. Gaikwad and J. Bang, "Hardness and Mechanical Properties of Wurtzite B–C–N Compounds," *Journal of Physical Chemistry C* 127, no. 5 (2023): 2581–2588.

[26] H. Wei, H. Zhan, D. Legut, and S. Zhang, "A Dislocation Perspective on Heterointerfacial Strengthening in Nanostructured Diamond and Cubic Boron Nitride Composites," *Carbon* 235 (2025): 120079.

[27] M. Li, Y. Zhou, B. Liu, et al., "A Wide-Bandgap Graphene-Like Structure C6BN With Ultra-Low Dielectric Constant," *Physical Chemistry Chemical Physics* 26, no. 26 (2024): 18302–18310.

[28] G. Christensen, D. Lou, H. Hong, and G. P. Peterson, "Improved Thermal Conductivity of Fluids and Composites Using Boron Nitride (BN) Nanoparticles through Hydrogen Bonding," *Thermochimica Acta* 700 (2021): 178927.

[29] Z. Shen, R. Dong, J. Li, Y. Su, and X. Long, "Determination of Gradient Residual Stress for Elastoplastic Materials by Nanoindentation," *Journal of Manufacturing Processes* 109 (2024): 359–366.

[30] X. Long, Y. Li, Z. Shen, Y. Su, T. Gu, and K. S. Siow, "Review of Uniqueness Challenge in Inverse Analysis of Nanoindentation," *Journal of Manufacturing Processes* 131 (2024): 1897–1916.

[31] G. Han, H. Cheng, C. He, Y. Feng, and C. Liu, "Silver Nanoparticles Bridging Segregated Hexagonal Boron Nitride Networks for Enhancing the Thermal Conductivity of Polystyrene Composites," *Composites Communications* 34 (2022): 101267.

[32] W. Han, C. Yuan, M. Chen, et al., "Anchoring Carbon Nanotubes to Boron Nitride Microrods for Enhancing the Thermal Conductivity of Polystyrene," *Ceramics International* 49, no. 2 (2023): 2140–2148.

[33] Q. Weng, X. Wang, X. Wang, Y. Bando, and D. Golberg, "Functionalized Hexagonal Boron Nitride Nanomaterials: Emerging Properties and Applications," *Chemical Society Reviews* 45, no. 14 (2016): 3989–4012.

[34] H. Chen, V. V. Ginzburg, J. Yang, et al., "Thermal Conductivity of Polymer-Based Composites: Fundamentals and Applications," *Progress in Polymer Science* 59 (2016): 41–85.

[35] C. Yu, W. Gong, J. Zhang, et al., "Hot Pressing-Induced Alignment of Hexagonal Boron Nitride in SEBS Elastomer for Superior Thermally Conductive Composites," *RSC Advances* 8, no. 45 (2018): 25835–25845.

[36] Q. Wang, X. Cheng, Y. Sun, et al., "A Synergetic Effect Between Photogenerated Carriers and Photothermally Enhanced Electrochemical Urea-Assisted Hydrogen Generation on the Ni-NiO/Nickel Foam Catalyst," *Materials Advances* 2, no. 6 (2021): 2104–2111.

[37] A. Rajput, S. K. Raj, J. Sharma, N. H. Rathod, P. D. Maru, and V. Kulshrestha, "Sulfonated Poly Ether Ether Ketone (SPEEK) Based Composite Cation Exchange Membranes for Salt Removal from Brackish Water," *Colloids and Surfaces A: Physicochemical and Engineering Aspects* 614 (2021): 126157.

[38] D. Zhang, Z. Jin, J. Shi, et al., "A Composite With a Gradient Distribution of Graphene and Its Anisotropic Electromagnetic Reflection," *RSC Advances* 10, no. 6 (2020): 3314–3318.

[39] J. Jose, Z. Ahmad, and S. Thomas, "Hybrid Nanoparticle-Based XLPE/SiO2/TiO2 and XLPE/SiO2 Nanocomposites: Nanoscale Hybrid Assembling," *Mechanics and Thermal Properties* (2014): 895–902.

[40] J. P. Jose and S. Thomas, "Alumina–Clay Nanoscale Hybrid Filler Assembling in Cross-Linked Polyethylene Based Nanocomposites: Mechanics and Thermal Properties," *Physical Chemistry Chemical Physics* 16, no. 28 (2014): 14730–14740.

[41] X. Zeng, L. Ye, S. Yu, et al., "Artificial Nacre-Like Papers Based on Noncovalent Functionalized Boron Nitride Nanosheets With Excellent Mechanical and Thermally Conductive Properties," *Nanoscale* 7, no. 15 (2015): 6774–6781.

[42] A. Nadeem, M. F. Maqsood, M. A. Raza, et al., "Thermally Stable and Anti-Corrosive Polydimethyl Siloxane Composite Coatings Based on Nanoforms of Boron Nitride," *Inorganic Chemistry Communications* 168 (2024): 112989.

[43] M. F. Maqsood, M. A. Raza, Z. U. Rehman, et al., "Role of Solvent Used in Development of Graphene Oxide Coating on AZ31B Magnesium Alloy: Corrosion Behavior and Biocompatibility Analysis," *Nanomaterials* 12, no. 21 (2022): 3745.

[44] H. Jiang, Y. Xie, M. He, et al., "Highly Thermally Conductiveand Flame-Retardant Waterborne Polyurethane Composites With 3D BNNS Bridging Structures via MagneticField Assistance," *Nano-Micro Letters* 17, no. 1 (2025): 138.

[45] H. Ma, B. Gao, M. Wang, et al., "Strategies for Enhancing Thermal Conductivity of Polymer-Based Thermal Interface Materials: A Review," *Journal of Materials Science* 56, no. 2 (2021): 1064–1086.

[46] S. Yu, X. Shen, and J.-K. Kim, "Beyond Homogeneous Dispersion: Oriented Conductive Fillers for High κ Nanocomposites," *Materials Horizons* 8, no. 11 (2021): 3009–3042.

[47] J. Qin, H. Lu, S. Yang, W. Su, and Y. Xing, "Research Progress in Dielectric Properties of Inorganic Two-Dimensional Nano-Fillers Polyvinylidene Fluoride Nano-Dielectric Materials," *Energy Technology* 12, no. 12 (2024): 2400967.

[48] A. T. Matveev, E. S. Permyakova, A. M. Kovalskii, et al., "New Insights into Synthesis of Nanocrystalline Hexagonal BN," *Ceramics International* 46, no. 12 (2020): 19866–19872.

[49] A. Nadeem, M. A. Raza, M. F. Maqsood, M. T. Ilyas, A. Westwood, and Z. U. Rehman, "Characterization of Boron Nitride Nanosheets Synthesized by Boron-Ammonia Reaction," *Ceramics International* 46, no. 12 (2020): 20415–20422.

[50] J. H. Kim, H. Cho, T. V. Pham, et al., "Dual Growth Mode of Boron Nitride Nanotubes in High Temperature Pressure Laser Ablation," *Scientific Reports* 9, no. 1 (2019): 15674.

[51] J. Ma, N. Luo, Z. Xie, F. Chen, and Q. Fu, "Preparation of Modified Hexagonal Boron Nitride by Ball-Milling and Enhanced Thermal Conductivity of Epoxy Resin," *Materials Research Express* 6, no. 10 (2019): 1050d8.

[52] Y. Bai, J. Zhang, Y. Wang, et al., "Ball Milling of Hexagonal Boron Nitride Microflakes in Ammonia Fluoride Solution Gives Fluorinated Nanosheets That Serve as Effective Water-Dispersible Lubricant Additives," *ACS Applied Nano Materials* 2, no. 5 (2019): 3187–3195.

[53] J. Liu, L. Yu, X. Cai, et al., "Sandwiching h-BN Monolayer Films Between Sulfonated Poly(ether ether Ketone) and Nafion for Proton Exchange Membranes With Improved Ion Selectivity," *ACS Nano* 13, no. 2 (2019): 2094–2102.

[54] Z. Li, Z. Wang, Q. Zhang, et al., "Research Progress on the Epitaxial Growth of Hexagonal Boron Nitride on Different Substrates by the CVD Method," *Nanoscale Advances* 7, no. 9 (2025): 2395–2417.

[55] M. Wang, H. Shi, S. Hussain, G. Liu, S.-Y. Lei, and N. Wan, "Study on the Failure Mechanism of Antioxidant on Copper Foils With Growing Hexagonal Boron Nitride Films," *Chemistry of Materials* 36, no. 12 (2024): 6205–6218.

[56] C. Gautam and S. Chelliah, "Methods of Hexagonal Boron Nitride Exfoliation and Its Functionalization: Covalent and Non-Covalent Approaches," *RSC Advances* 11, no. 50 (2021): 31284–31327.

[57] L. Zhao, L. Yan, C. Wei, et al., "Aqueous-Phase Exfoliation and Functionalization of Boron Nitride Nanosheets Using Tannic Acid for Thermal Management Applications," *Industrial and Engineering Chemistry Research* 59, no. 37 (2020): 16273–16282.

[58] N. G. Chopra, R. J. Luyken, K. Cherrey, et al., "Boron Nitride Nanotubes," *Science* 269, no. 5226 (1995): 966-967.

[59] E. A. Turhan, A. E. Pazarçeviren, Z. Evis, and A. Tezcaner, "Properties and Applications of Boron Nitride Nanotubes," *Nanotechnology* 33, no. 24 (2022): 242001.

[60] G. Dominguez-Rodríguez, G. Canto, C. Cab, J. Medina, and J. A. Tapia, "Strong Stretching Bond Force Constants and Young's Moduli in Boron Nitride Nanotubes," *Solid State Communications* 395 (2025): 115734.

[61] L. Zhao, C. Wei, Z. Li, et al., "High-Temperature Dielectric Paper With High Thermal Conductivity and Mechanical Strength by Engineering the Aramid Nanofibers and Boron Nitride Nanotubes," *Materials and Design* 210 (2021): 110124.

[62] J. Shim, D. I. Son, J. S. Lee, et al., "BNNT-ZnO QDs Nanocomposites for Improving Piezoelectric Nanogenerator and Piezoelectric Properties of Boron Nitride Nanotube," *Nano Energy* 93 (2022): 106886.

[63] C. M. Lee, S. I. Choi, S. S. Choi, and S. H. Hong, "Synthesis of Boron Nitride Nanotubes by Arc-Jet Plasma," *Current Applied Physics* 6, no. 2 (2006): 166–170.

[64] P. Ahmad, M. U. Khandaker, Z. R. Khan, and Y. M. Amin, "Synthesis of Boron Nitride Nanotubes Via Chemical Vapour Deposition: A Comprehensive Review," *RSC Advances* 5, no. 44 (2015): 35116–35137.

[65] D. Bae, K.-H. Lee, and M. J. Kim, "Growth Methodologies of Boron Nitride Nanotubes and Their Neutron Shielding Applications: A Review," *Nanoscale* 16, no. 8 (2024): 3817–3837.

[66] L. H. Li, Y. Chen, and A. M. Glushenkov, "Synthesis of Boron Nitride Nanotubes by Boron Ink Annealing," *Nanotechnology* 21, no. 10 (2010): 105601.

[67] V. G. Naumov, F. K. Kosyrev, V. G. Vostrikov, et al., "Synthesis of Boron Nitride Multi-Walled Nanotubes by Laser Ablation Technique," *Laser Physics* 19, no. 5 (2009): 1198–1200.

[68] C. Zhuang, H. Xu, L. Li, Y. Liu, C. Ban, and X. Liu, "Systematic Investigation of the Ball Milling–Annealing Growth and Electrical Properties of Boron Nitride Nanotubes," *RSC Advances* 6, no. 114 (2016): 113415–113423.

[69] P. Ahmad, M. U. Khandaker, Y. M. Amin, et al., "Synthesis of Hexagonal Boron Nitride Fibers Within 2 h Annealing at 500°C and 2 h Growth Duration at 1000°C," *Ceramics International* 42, no. 13 (2016): 14661–14666.

[70] P. Ahmad, M. Uddin Khandaker, Y. Mohd Amin, M. Amin, M. Imran Irshad, and I. Ud Din, "Low Temperature Synthesis of High Quality BNNTs Via Argon Supported Thermal CVD," *Ceramics International* 41, no. 10 (2015): 15222–15226.

[71] Y. Kim and J. Choi, "Electromechanical Origin of Phonon Dynamics Exhibiting Tunable Anisotropic Heat Transport in Layered Nanostructures," *Small Methods* 8, no. 3 (2024): 2301200.

[72] S. Li, H. Liu, Y. Xu, et al., "Aqueous Solution-Assisted In-Situ Polymerization for Fabrication of BNNS/PA12T Nanocomposites With Excellent Thermal Conductivity and Mechanical Properties," *Polymer Composites* 46, no. 4 (2025): 3732–3741.

[73] W. Yang, J. Kim, P.-C. Su, and J. Kim, "Improving the Thermal Conductivity of an Epoxy Composite With Chemically Boron Nitride-Grafted Carbon Fiber," *Composites Part A: Applied Science and Manufacturing* 182 (2024): 108192.

[74] A. Q. Abdullah, S. I. Hussein, N. A. Ali, et al., "A Comparative Study on the Effects of Multi-Walled Carbon Nanotubes and Graphene Nanoplates Incorporated for Improved Thermal Conductivity and Dielectric Properties of Polyvinyl Chloride," *Diamond and Related Materials* 145 (2024): 111143.

[75] H. Wang, W. Xing, S. Chen, C. Song, M. D. Dickey, and T. Deng, "Liquid Metal Composites With Enhanced Thermal Conductivity and Stability Using Molecular Thermal Linker," *Advanced Materials* 33, no. 43 (2021): 2103104.

[76] L. N. Rout, D. Mishra, and P. T. R. Swain, "Physical, Thermal, and Mechanical Characterization of Ceramic (SiC) Filled Woven Glass Fiber Reinforced Hybrid Polymer Composites," *Silicon* 16, no. 4 (2024): 1731–1741.

[77] H.-A. Cha, S.-J. Ha, M.-G. Jo, et al., "Three-Dimensional MgO Filler Networking Composites With Significantly Enhanced Thermal Conductivity," *Advanced Composites and Hybrid Materials* 7, no. 5 (2024): 178.

[78] Y. Srivastava and A. Jain, "Accelerating Thermal Conductivity Prediction Through Machine-Learning: Two Orders of Magnitude Reduction in Phonon-Phonon Scattering Rates Calculation," *Materials Today Physics* 41 (2024): 101345.

[79] Y. Wang, W. Zhang, M. Feng, et al., "The Influence of Boron Nitride Shape and Size on Thermal Conductivity, Rheological and Passive Cooling Properties of Polyethylene Composites," *Composites Part A: Applied Science and Manufacturing* 161 (2022): 107117.

[80] Z. Kuang, Y. Chen, Y. Lu, et al., "Fabrication of Highly Oriented Hexagonal Boron Nitride Nanosheet/Elastomer Nanocomposites With High Thermal Conductivity," *Small* 11, no. 14 (2015): 1655–1659.

[81] J. Xiang and L. T. Drzal, "Investigation of exfoliated Graphite Nanoplatelets (xGnP) in Improving Thermal Conductivity of Paraffin Wax-Based Phase Change Material," *Solar Energy Materials and Solar Cells* 95, no. 7 (2011): 1811–1818.

[82] H. Ishida and S. Rimdusit, “Very High Thermal Conductivity Obtained by Boron Nitride-Filled Polybenzoxazine,” *Thermochimica Acta* 320, no. 1-2 (1998): 177–186.

[83] S. Shaybanizadeh and A. Najafi Chermahini, “Fabricating Boron Nitride Nanosheets from Hexagonal BN in Water Solution by a Combined Sonication and Thermal-Assisted Hydrolysis Method,” *Ceramics International* 47, no. 8 (2021): 11122–11128.

[84] L. Wu, N. Luo, Z. Xie, Y. Liu, F. Chen, and Q. Fu, “Improved Breakdown Strength of Poly(vinylidene Fluoride)-Based Composites by Using All Ball-Milled Hexagonal Boron Nitride Sheets Without Centrifugation,” *Composites Science and Technology* 190 (2020): 108046.

[85] L. Cao, J. Wang, J. Dong, X. Zhao, H.-B. Li, and Q. Zhang, “Preparation of Highly Thermally Conductive and Electrically Insulating PI/BNNSs Nanocomposites by Hot-Pressing Self-Assembled PI/BNNSs Microspheres,” *Composites Part B: Engineering* 188 (2020): 107882.

[86] S. Wang, J. Tang, H. Xiang, et al., “Preparation of Functionalized Boron Nitride Nanosheets by One-Step Method for Improving the Thermal Conductivity of Polymers,” *Colloid and Interface Science Communications* 59 (2024): 100776.

[87] W. Meng, Y. Huang, Y. Fu, Z. Wang, and C. Zhi, “Polymer Composites of Boron Nitride Nanotubes and Nanosheets,” *Journal of Materials Chemistry C* 2, no. 47 (2014): 10049–10061.

[88] M. E. Mackay, A. Tuteja, P. M. Duxbury, et al., “General Strategies for Nanoparticle Dispersion,” *Science* 311, no. 5768 (2006): 1740–1743.

[89] W. Zhou, C. Wang, T. Ai, K. Wu, F. Zhao, and H. Gu, “A Novel Fiber-Reinforced Polyethylene Composite With Added Silicon Nitride Particles for Enhanced Thermal Conductivity,” *Composites Part A: Applied Science and Manufacturing* 40, no. 6-7 (2009): 830–836.

[90] S. Li, S. Qi, N. Liu, and P. Cao, “Study on Thermal Conductive BN/Novolac Resin Composites,” *Thermochimica Acta* 523, no. 1-2 (2011): 111–115.

[91] W. Zhou, S. Qi, H. Li, and S. Shao, “Study on Insulating Thermal Conductive BN/HDPE Composites,” *Thermochimica Acta* 452, no. 1 (2007): 36–42.

[92] S. Ghaffari Mosanenzadeh and H. E. Naguib, “Effect of Filler Arrangement and Networking of Hexagonal Boron Nitride on the Conductivity of New Thermal Management Polymeric Composites,” *Composites Part B: Engineering* 85 (2016): 24–30.

[93] H. Liu, X. Su, R. Fu, B. Wu, and X. Chen, “The Flexible Film of SCF/BN/PDMS Composites With High Thermal Conductivity and Electrical Insulation,” *Composites Communications* 23 (2021): 100573.

[94] W. Han, M. Chen, W. Song, C. Ge, and X. Zhang, “Construction of Hexagonal Boron Nitride@polystyrene Nanocomposite With High Thermal Conductivity for Thermal Management Application,” *Ceramics International* 46, no. 6 (2020): 7595–7601.

[95] K. Kim and J. Kim, “Vertical Filler Alignment of Boron Nitride/Epoxy Composite for Thermal Conductivity Enhancement via External Magnetic Field,” *International Journal of Thermal Sciences* 100 (2016): 29–36.

[96] G. Zou, K. Xiong, C. Jiang, et al., “Magnetic Fe3O4 Nanodisc Synthesis on a Large Scale via a Surfactant-Assisted Process,” *Nanotechnology* 16, no. 9 (2005): 1584–1588.

[97] K. Kim and J. Kim, “Fabrication of Thermally Conductive Composite With Surface Modified Boron Nitride by Epoxy Wetting Method,” *Ceramics International* 40, no. 4 (2014): 5181–5189.

[98] N. Sun, J. Sun, X. Zeng, et al., “Hot-Pressing Induced Orientation of Boron Nitride in Polycarbonate Composites With Enhanced Thermal Conductivity,” *Composites Part A: Applied Science and Manufacturing* 110 (2018): 45–52.

[99] H. Zhu, Y. Li, Z. Fang, et al., “Highly Thermally Conductive Papers With Percolative Layered Boron Nitride Nanosheets,” *ACS Nano* 8, no. 4 (2014): 3606–3613.

[100] N. Burger, A. Laachachi, M. Ferriol, M. Lutz, V. Toniazzo, and D. Ruch, “Review of Thermal Conductivity in Composites: Mechanisms, Parameters and Theory,” *Progress in Polymer Science* 61 (2016): 1–28.

[101] W. Dai, Y. Wang, M. Li, et al., “2D Materials-Based Thermal Interface Materials: Structure, Properties, and Applications,” *Advanced Materials* 36, no. 37 (2024): 2311335.

[102] K. Zhan, Y. Chen, Z. Xiong, et al., “Low Thermal Contact Resistance Boron Nitride Nanosheets Composites Enabled by Interfacial Arc-Like Phonon Bridge,” *Nature Communications* 15, no. 1 (2024): 2905.

[103] J. Jin, Y. Su, J. Guo, et al., “Flexible Composite Films With Ultrahigh through-Plane Thermal Conductivity yet Low Graphene Content,” *Composites Part B: Engineering* 286 (2024): 111780.

[104] Y. Dong, H. Yu, Y. Feng, and W. Feng, “Structure, Properties and Applications of Multi-Functional Thermally Conductive Polymer Composites,” *Journal of Materials Science & Technology* 200 (2024): 141–161.

[105] S. Dong, M. Zhang, K. Jin, and R. Yang, “An Improved Laser Flash Method for Thermal Conductivity Measurement of Molten Salts,” *Progress in Natural Science: Materials International* 34, no. 2 (2024): 345–353.

[106] H. Liu, Z. Chai, K. Wei, et al., “A Study on the Thermal Conductivity of Proton Irradiated CVD-SiC and Sintered SiC, Measured Using a Modified Laser Flash Method With Multi-Step Machining,” *Journal of the European Ceramic Society* 44, no. 11 (2024): 6305–6320.

[107] J.-G. Bauzin and N. Laraqi, “New Thermal Analysis of the Hot Disc Method Based on Explicit Analytical Developments,” *International Journal of Thermal Sciences* 195 (2024): 108645.

[108] S. E. Gustafsson, B. M. Mihiretie, and M. K. Gustavsson, “Measurement of Thermal Transport in Solids With the Hot Disc Method,” *International Journal of Thermophysics* 45, no. 1 (2024): 1.

[109] L. Zhang, H. Kong, and H. Zheng, “Numerical Manifold Method for Steady-State Nonlinear Heat Conduction Using Kirchhoff Transformation,” *Science China Technological Sciences* 67, no. 4 (2024): 992–1006.

[110] S. Qiao, Y. Tao, and L. Yang, “Negative Correlation Between Cross-Plane Bonding Strength and In-Plane Thermal Transport in Bent Van der Waals Materials,” *Physical Review B* 110, no. 24 (2024): 245411.

[111] G. Zhang, S. Xue, F. Chen, and Q. Fu, “An Efficient Thermal Interface Material With Anisotropy Orientation and High Through-Plane Thermal Conductivity,” *Composites Science and Technology* 231 (2023): 109784.

[112] K. Zheng and X. Tian, *Characterization Methods for Thermal Management Materials, in Thermal Management Materials for Electronic Packaging* (John Wiley & Sons, Ltd., 2024): 39–76.

[113] M. Mirković-Marjanović, A. Kijanović, S. Ilić, K. Janković, and D. Zakić, “Verification and Validation of an Advanced

Guardedhot Plate for Determination of Thermal Conductivity," *Thermal Science* 26, no. 6 Part A (2022): 4735–4747.

[114] H.-P. Ebert and S. Vidi, "Correct Use of the Guarded-Hot-Plate Method for Thermal Conductivity Measurements on Solids," *International Journal of Thermophysics* 45, no. 2 (2024): 20.

[115] S. Tarasovs and A. Aniskevich, "Identification of the Anisotropic Thermal Conductivity by an Inverse Solution Using the Transient Plane Source Method," *Measurement* 206 (2023): 112252.

[116] S. Malinarič and A. Elkholy, "Comparison of the New Plane Source Method to the Step Wise Transient Method for Thermal Conductivity and Diffusivity Measurement," *International Journal of Thermal Sciences* 164 (2021): 106901.

[117] A. Zandieh, P. Buahom, E. Baradaran Shokouhi, et al., "Highly Anisotropic Thermally Conductive Dielectric Polymer/Boron Nitride Nanotube Composites for Directional Heat Dissipation," *Small* 20, no. 48 (2024): 2404189.

[118] B. Wei, W. Luo, J. Du, et al., "Thermal Interface Materials: From Fundamental Research to Applications," *SusMat* 4, no. 6 (2024): e239.

[119] Y. Lin, P. Li, W. Liu, et al., "Application-Driven High-Thermal-Conductivity Polymer Nanocomposites," *ACS Nano* 18, no. 5 (2024): 3851–3870.

[120] H. J. Mun, H.-B. Cho, and Y.-H. Choa, "High Quasi-Isotropic Thermal Conductivity of Polydimethylsiloxane Nanocomposites With Hexagonal-Boron Nitride Microspheres and Flakes," *ACS Applied Polymer Materials* 6, no. 9 (2024): 5058–5069.

[121] L. An, Y. Yu, Q. Cai, S. Mateti, L. H. Li, and Y. I. Chen, "Hexagonal Boron Nitride Nanosheets: Preparation, Heat Transport Property and Application as Thermally Conductive Fillers," *Progress in Materials Science* 138 (2023): 101154.

[122] G. Liu, A. Ding, P. Xu, et al., "Thermal Conductivity of Epoxy Composites Containing 3D Honeycomb Boron Nitride Filler," *Chemical Engineering Journal* 489 (2024): 151170.

[123] B. Hu, H. Guo, Q. Wang, et al., "Enhanced Thermal Conductivity by Constructing 3D-Networks in Poly(vinylidene Fluoride) Composites Via Positively Charged Hexagonal Boron Nitride and Silica Coated Carbon Nanotubes," *Composites Part A: Applied Science and Manufacturing* 137 (2020): 106038.

[124] M. Kundu, C. M. Costa, J. Dias, A. Maceiras, J. L. Vilas, and S. Lanceros-Méndez, "On the Relevance of the Polar β-Phase of Poly(vinylidene Fluoride) for High Performance Lithium-Ion Battery Separators," *Journal of Physical Chemistry C* 121, no. 47 (2017): 26216–26225.

[125] S.-Y. Yang, C.-C.M. Ma, C.-C. Teng, et al., "Effect of Functionalized Carbon Nanotubes on the Thermal Conductivity of Epoxy Composites," *Carbon* 48, no. 3 (2010): 592–603.

[126] W. Yu, J. Fu, L. Chen, et al., "Enhanced Thermal Conductive Property of Epoxy Composites by Low Mass Fraction of Organic–Inorganic Multilayer Covalently Grafted Carbon Nanotubes," *Composites Science and Technology* 125 (2016): 90–99.

[127] J. Hansson, T. M. J. Nilsson, L. Ye, and J. Liu, "Novel Nanostructured Thermal Interface Materials: A Review," *International Materials Reviews* 63, no. 1 (2017): 22–45.

[128] V. Talesara, PaulD. Garman, J. L. Lee, and W. Lu, "Thermal Management of High-Power Switching Transistors Using Thick CVD-Grown Graphene Nanomaterial," *IEEE Transactions on Power Electronics* 35, no. 1 (2020): 578–590.

[129] W. Yang, N.-N. Wang, P. Ping, et al., "Novel 3D Network Architectured Hybrid Aerogel Comprising Epoxy, Graphene, and Hydroxylated Boron Nitride Nanosheets," *ACS Applied Materials & Interfaces* 10, no. 46 (2018): 40032–40043.

[130] J. Han, G. Du, W. Gao, and H. Bai, "An Anisotropically High Thermal Conductive Boron Nitride/Epoxy Composite Based on Nacre-Mimetic 3D Network," *Advanced Functional Materials* 29, no. 13 (2019): 1900412.

[131] M. Cao, C. Du, H. Guo, S. Song, X. Li, and B. Li, "Continuous Network of CNTs in Poly(vinylidene Fluoride) Composites With High Thermal and Mechanical Performance for Heat Exchangers," *Composites Science and Technology* 173 (2019): 33–40.

[132] J. Chen, X. Huang, Y. Zhu, and P. Jiang, "Cellulose Nanofiber Supported 3D Interconnected BN Nanosheets for Epoxy Nanocomposites With Ultrahigh Thermal Management Capability," *Advanced Functional Materials* 27, no. 5 (2017): 1604754.

[133] I. Jo, M. T. Pettes, J. Kim, et al., "Thermal Conductivity and Phonon Transport in Suspended Few-Layer Hexagonal Boron Nitride," *Nano Letters* 13, no. 2 (2013): 550–554.

[134] J. Cai, S. Kimura, M. Wada, S. Kuga, and L. Zhang, "Cellulose Aerogels from Aqueous Alkali Hydroxide–Urea Solution," *ChemSusChem* 1, no. 1-2 (2008): 149–154.

[135] S. Wang, A. Lu, and L. Zhang, "Recent Advances in Regenerated Cellulose Materials," *Progress in Polymer Science* 53 (2016): 169–206.

[136] Z. Yin, J. Guo, and X. Jiang, "Significantly Improved Thermal Conductivity of Silicone Rubber and Aligned Boron Nitride Composites by a Novel Roll-Cutting Processing Method," *Composites Science and Technology* 209 (2021): 108794.

[137] Y. Xue, X. Li, H. Wang, F. Zhao, D. Zhang, and Y. Chen, "Improvement in Thermal Conductivity of Through-Plane Aligned Boron Nitride/Silicone Rubber Composites," *Materials and Design* 165 (2019): 107580.

[138] Y. Ji, S.-D. Han, H. Wu, S.-Y. Guo, F.-S. Zhang, and J.-H. Qiu, "Understanding the Thermal Impedance of Silicone Rubber/Hexagonal Boron Nitride Composites as Thermal Interface Materials," *Chinese Journal of Polymer Science* 42, no. 3 (2024): 352–363.

[139] H. Dong, Z. Liu, J. Guo, S. Lv, H. Huang, and X. Jiang, "Vertically Aligned Carbon Fiber/Polydimethylsiloxane Composites Prepared by Lyophilization With Exceptional Thermal Conductivity and Electromagnetic Interference Shielding Performance," *Chemical Engineering Journal* 490 (2024): 151620.

[140] R. Zhang, Z. Liu, Z. Sun, et al., "A Scalable Highly Thermal Conductive Silicone Rubber Composite With Orientated Graphite by Pre-Vulcanizing and Multilayer Stacking Method," *Composites Part A: Applied Science and Manufacturing* 157 (2022): 106944.

[141] W. Wu, M. Zheng, K. Lu, et al., "Thermally Conductive Composites Based on Hexagonal Boron Nitride Nanosheets for Thermal Management: Fundamentals to Applications," *Composites Part A: Applied Science and Manufacturing* 169 (2023): 107533.

[142] M. G. Rasul, A. Kiziltas, B. Arfaei, and R. Shahbazian-Yassar, "2D Boron Nitride Nanosheets for Polymer Composite Materials," *NPJ 2D Materials and Applications* 5, no. 1 (2021): 1–18.

[143] F. Wang, X. Dong, G. Liu, et al., "Covalent Bond-Assisted Continuous Interface Structure for High Thermal Conductive Polyimide Composite Films," *Composites Part A: Applied Science and Manufacturing* 185 (2024): 108348.

[144] C. Jia, P. Zhang, S. M. Seraji, et al., "Effects of BN/GO on the Recyclable, Healable and Thermal Conductivity Properties of ENR/PLA Thermoplastic Vulcanizates," *Composites Part A: Applied Science and Manufacturing* 152 (2022): 106686.

[145] D. An, S. Cheng, S. Xi, et al., "Flexible Thermal Interfacial Materials With Covalent Bond Connections for Improving High Thermal Conductivity," *Chemical Engineering Journal* 383 (2020): 123151.

[146] A. Bashir, M. Maqbool, R. Lv, et al., "Engineering of Interfacial Interactions Among BN and CNT Hybrid Towards Higher Heat Conduction Within TPU Composites," *Composites Part A: Applied Science and Manufacturing* 167 (2023): 107428.

[147] H. Cheng, K. Zhao, Y. Gong, et al., "Covalent Coupling Regulated Thermal Conductivity of Poly(vinyl Alcohol)/Boron Nitride Composite Film Based on Silane Molecular Structure," *Composites Part A: Applied Science and Manufacturing* 137 (2020): 106026.

[148] X. Yang, Y. Guo, Y. Han, et al., "Significant Improvement of Thermal Conductivities for BNNS/PVA Composite Films *via* Electrospinning Followed by Hot-Pressing Technology," *Composites Part B: Engineering* 175 (2019): 107070.

[149] R. Wang, H. Cheng, Y. Gong, et al., "Highly Thermally Conductive Polymer Composite Originated from Assembly of Boron Nitride at an Oil–Water Interface," *ACS Applied Materials & Interfaces* 11, no. 45 (2019): 42818–42826.

[150] S. Lin and M. J. Buehler, "The Effect of Non-Covalent Functionalization on the Thermal Conductance of Graphene/Organic Interfaces," *Nanotechnology* 24, no. 16 (2013): 165702.

[151] J. Hong, J. Lee, C. K. Hong, and S. E. Shim, "Effect of Dispersion State of Carbon Nanotube on the Thermal Conductivity of Poly(dimethyl Siloxane) Composites," *Current Applied Physics* 10, no. 1 (2010): 359–363.

[152] K. Zhang, C. Chen, Y. Wen, et al., "Directional Thermal Transport Feature in Binary Filler-Based SiR Composites With Horizontally Oriented h-BN," *Composites Science and Technology* 254 (2024): 110666.

[153] L. Liang, Y. Feng, K. Yang, Z. Zhang, and Q. Chen, "Thermally Conductive h-BN/EP Composites Oriented by AC Electric Field Induction," *International Journal of Heat and Mass Transfer* 225 (2024): 125397.

[154] H. Niu, H. Guo, L. Kang, et al., "Highly Thermally Conductive and Soft Thermal Interface Materials Based on Vertically Oriented Boron Nitride Film," *Composites Part B: Engineering* 272 (2024): 111219.

[155] S. Zhou, T. Xu, N. Song, J. Dai, G. Qian, and P. Ding, "Oriented BN/BNNT Heterostructure Constructed by Interface Engineering Strategy for Polyamide-Imide Composite Film With Advanced Flexibility and Thermally Conductive Properties," *Chemical Engineering Journal* 481 (2024): 148653.

[156] X. Hou, Y. Chen, W. Dai, et al., "Highly Thermal Conductive Polymer Composites Via Constructing Micro-Phragmites Communis Structured Carbon Fibers," *Chemical Engineering Journal* 375 (2019): 121921.

[157] H. Jiang, Z. Wang, H. Geng, X. Song, H. Zeng, and C. Zhi, "Highly Flexible and Self-Healable Thermal Interface Material Based on Boron Nitride Nanosheets and a Dual Cross-Linked Hydrogel," *ACS Applied Materials & Interfaces* 9, no. 11 (2017): 10078–10084.

[158] K. Yang, X. Yang, Z. Liu, et al., "Vertically Aligned Boron Nitride Nanosheets Films for Superior Electronic Cooling," *ACS Applied Materials & Interfaces* 15, no. 23 (2023): 28536–28545.

[159] K. Özdoğan and S. Berber, "Optimizing the Hydrogen Storage in Boron Nitride Nanotubes by Defect Engineering," *International Journal of Hydrogen Energy* 34, no. 12 (2009): 5213–5217.

[160] P. M. Revabhai, R. K. Singhal, H. Basu, and S. K. Kailasa, "Progress on Boron Nitride Nanostructure Materials: Properties, Synthesis and Applications in Hydrogen Storage and Analytical Chemistry," *Journal of Nanostructure in Chemistry* 13, no. 1 (2023): 1–41.